



## Research article

# The mysteries of pharmacokinetics and *in vivo* metabolism of *Oroxylum indicum* (L.) Kurz: A new perspective from MSOP method

Xia Zhang<sup>a</sup>, Yuan Zhang<sup>a</sup>, Na Wang<sup>b</sup>, Jian Liu<sup>a</sup>, Lan-tong Zhang<sup>c</sup>,  
Zhi-qing Zhang<sup>a</sup>, De-qiang Li<sup>a,\*</sup>

<sup>a</sup> Department of Pharmacy, the Second Hospital of Hebei Medical University, Shijiazhuang, 050000, Hebei province, China

<sup>b</sup> Maternal and Child Health Hospital of Gucheng County, Hengshui, China

<sup>c</sup> Department of Pharmaceutical Analysis, School of Pharmacy, Hebei Medical University, China

## ARTICLE INFO

## Keywords:

*Oroxylum indicum* (L.) Kurz  
Metabolites  
MSOP method  
Pharmacokinetic study  
UHPLC-Q-TOF/MS

## ABSTRACT

The pharmacological effects of flavonoids in *Oroxylum indicum* (L.) Kurz against inflammation, bacterial, and oxidation have been well-documented. Additionally, it is commonly consumed as tea. However, the *in vivo* mechanism of its main compounds has not been well elucidated. In this study, a highly selective and sensitive UHPLC-Q-TOF-MS method combined with Mass Spectrum-based Orthogonal Projection (MSOP) theory and four-step analytical strategy was established and validated to identify metabolites in rats following oral administration *Oroxylum indicum* (L.) Kurz extract. Furthermore, a sensitive LC-MS/MS method was developed and validated for the first time to analyze the pharmacokinetics of ten main flavonoids in rats. Notably, a total of 47 metabolites were identified in blood, bile, urine, and feces samples. The maximum plasma concentration ( $C_{max}$ ) values for oroxin A, oroxin B, baicalin, chrysin, baicalein, scutellarein, apigenin, quercetin oroxylin A and isorhamnetin were  $2945.1 \pm 11.23$  ng/mL,  $3123.9 \pm 16.37$  ng/mL,  $130.40 \pm 27.52$  ng/mL,  $117.20 \pm 28.54$  ng/mL,  $64.12 \pm 19.33$  ng/mL,  $97.22 \pm 24.27$  ng/mL,  $145.22 \pm 29.92$  ng/mL,  $45.19 \pm 18.84$  ng/mL,  $67.32 \pm 15.78$  ng/mL and  $128.44 \pm 26.42$  ng/mL. A double peak was observed in the drug-time curve of apigenin, due to enterohepatic recirculation. This study demonstrated that MSOP method provided more technical support for the identification of flavonoid metabolites in complex system than traditional methods.

## 1. Introduction

*Oroxylum indicum* (L.) Kurz, also known as Laminated paper, *Oroxylum indicum* and so on, is the mature seed of Bignoniaceae *Oroxylum* Vent [1–3]. As a widely used traditional Chinese medicine, *Oroxylum indicum* (L.) Kurz boasts a medicinal legacy spanning centuries. It has been employed in the treatment of upper respiratory infections, acute bronchitis, chronic pharyngitis pneumonia and other related ailments [4]. Modern pharmacological studies have demonstrated that the primary pharmacodynamic constituents of *Oroxylum indicum* (L.) Kurz are flavonoids, which exhibit anti-inflammatory [5], antioxidant [6], hypoglycemic [7], anti-virus [8], and anti-tumor growth [9] properties. *Oroxylum indicum* (L.) Kurz predominantly thrives in Nepal, India and China (with Guangdong,

\* Corresponding author.

E-mail address: [lidgeqiang@hebmh.edu.cn](mailto:lidgeqiang@hebmh.edu.cn) (D.-q. Li).

<https://doi.org/10.1016/j.heliyon.2024.e33234>

Received 22 January 2024; Received in revised form 17 June 2024; Accepted 17 June 2024

Available online 19 June 2024

2405-8440/© 2024 The Authors. Published by Elsevier Ltd. This is an open access article under the CC BY-NC license (<http://creativecommons.org/licenses/by-nc/4.0/>).

Guangxi, Guizhou, and Yunnan provinces being the most abundant sources) [10]. As a traditional medicinal herb, it is extensively utilized in Eastern countries [11].

Metabolites samples often contain a plethora of prototype compounds and endogenous metabolites, particularly complex components derived from medicinal materials that remain unidentified. Consequently, distinguishing them from the metabolites *in vivo* becomes challenging [12–14], thereby significantly impacting the accuracy of medicinal material metabolism results [15], and leading to an unclear understanding of the pharmacodynamic material basis *in vivo* [16,17]. Traditional studies on the *in vivo* metabolism of medicinal have typically relied on analyzing the metabolic pathways of representative components and predicting metabolites for similar components to evaluate the efficacy of traditional Chinese medicine metabolism, or comparing chemical fingerprints of plant materials with metabolite profiles to identify *in vivo* metabolites [18–20]. However, these traditional methods involve complex data processing, large sample size, and procedures. Therefore, it is crucial to establish a robust and comprehensive strategy for identifying multi-component metabolites in traditional Chinese medicine.

Based on the orthogonality of mass spectrum signals, a new method (Mass Spectrum-based Orthogonal Projection, MSOP) was established to eliminate the interference of exogenous metabolites. Initially, the conditions of the method were investigated by simulating LC-MS data. Subsequently, the validity and feasibility of the method were verified by using standard sample data. All comprehensive investigations and verifications unequivocally demonstrated that the MSOP method could successfully capture and eliminate interference signals arising from exogenous metabolites. Furthermore, leveraging the orthogonality of mass spectrum signals as a new baseline drift correction method was proposed, which could obtain the real chromatographic baseline.

Pharmacokinetics (PK) is a quantitative subject area that studies the *in vivo* process of drug, including absorption, distribution, metabolism and excretion. It employs mathematical principles and methods to elaborate on the dynamic regulation of drugs *in vivo* [21]. The determination of drug dosage and interval is based on whether the drug can achieve a safe and effective concentration at its site of action [22]. Due to internal processes, the drug's concentration at the site of action varies dynamically [23]. For developing innovative drugs, pharmacokinetics, pharmacodynamics and toxicology studies are equally important and have become an integral part of preclinical and clinical research. However, the PK study for multi-components in *Oroxylum indicum* (L.) Kurz has not been applied.

The present study describes the application of an orthogonal projection of MSOP for investigating *in vivo* metabolism of *Oroxylum indicum* (L.) Kurz (seed of *Oroxylum indicum* (L.) Kurz) [24–26]. The theory and mathematical algorithm underlying MSOP are presented, along with its successful implementation for rapid screening and characterization of flavonoid metabolites in *Oroxylum indicum* (L.) Kurz. A total of 47 metabolites were identified based on tandem MS spectra and Clog P values. These findings reveal invaluable technical support and new insights into the identification of flavonoid metabolites within intricate systems of traditional Chinese medicine by demonstrating the efficacy of the MSOP method in removing interfering components during rat metabolism studies on medicinal materials. Additionally, a novel HPLC-MS/MS method was developed to simultaneously determine ten compounds in rat plasma following oral administration of *Oroxylum indicum* (L.) Kurz extract. Pharmacokinetic parameters were summarized, whereby the results of this investigation present a strong foundation for the future clinical implementation.

## 2. Materials and methods

### 2.1. Chemicals and materials

Oroxin A (DST201203-028), oroxin B (DST200918-029), baicalin (110715–200514), chrysin (DST200323-048), baicalein (DSTDH002401), scutellarein (DST210512-030), apigenin (DSTDQ002601) and oroxylin A (DST180328-041) were purchased from Chengdu Desite Biotechnology Co. LTD. Baicalin (110715–200514) and quercetin (100081–200406) were purchased from National Institute for Food and Drug Control. Isorhamnetin (110860–201611) and sulfamethoxazole (100025–200904) were purchased from the National Institutes for Food and Drug Control. The contents of these standards were higher than 98 %. HPLC-grade methanol and acetonitrile were purchased from J.T. Baker Chemical Company (Phillipsburg, NJ, USA). Formic acid (HPLC grade) was provided by Diamond Technology (Dikma Technologies Inc., Lake Forest, CA, USA).

### 2.2. Instrumentation and conditions

UHPLC-Q-TOF-MS/MS coupled with a triple TOF™ 5600<sup>+</sup> MS/MS system (AB Sciex, CA, USA) was performed on a Shimadzu UHPLC system (Shimadzu Corp., Kyoto, Japan). Information-dependent acquisition (IDA) was used. Poroshell 120 EC-C<sub>18</sub> (2.1 × 100 mm, 2.7 μm) column with a SecurityGuard® UHPLC C<sub>18</sub> pre-column (Agilent Corp, Santa Clara, CA, USA) was used to separate chemical composition. The column temperature was set at 30 °C. Formic acid (0.1 %, A) and acetonitrile (B) consisted of mobile phase. The gradient elution program was performed as follows: 5–17 % B (0–1 min), 17–35 % B (1–3 min), 35–95 % B (3–12 min), and finally held at 95 % B for an additional 5 min. The mobile phase flow rate was set to 0.3 mL/min, while the injection volume was maintained at a constant value of 3 μL.

HPLC-MS/MS coupled with API 4000<sup>+</sup> MS/MS system (AB Sciex, CA, USA). Symmetry® C<sub>18</sub> (4.6 × 150 mm, 3.5 μm) column with a SecurityGuard® HPLC C<sub>18</sub> pre-column (Agilent Corp, Santa Clara, CA, USA) was used, and the column temperature was maintained at 25 °C. The mobile phase was made of water containing 0.1 % formic acid (A) and acetonitrile (B). The optimized gradient elution program was as follows: 35–45 % B from 0 to 2 min, followed by a linear from 45 % to 95 % B over the next 7 min. The mobile phase flow rate was set at a constant value of 0.8 mL/min, and the injection volume was maintained at 10 μL.

The operating conditions for the ESI interface were as follows: the ion spray voltage was set to –4.5 kV; the turbo spray temperature

was 650 °C; nebuliser gas (gas 1) and heater gas (gas 2) were set to 60 and 65 arbitrary units, respectively; the curtain gas was kept at arbitrary units and interface heater was on. Nitrogen was used in all cases. The retention time, characteristic MS/MS fragment ions data, declustering potential (DP) and collision energy (CE) for each analyte are listed in Table 1. Instrument control, data acquisition and evaluation were performed with Analyst 1.6.2 software (AB SCIEX, Ontario, Canada).

### 2.3. Preparation of *Oroxylum indicum* (L.) Kurz extract

Materials of *Oroxylum indicum* (L.) Kurz (Guangdong) was cut into pieces and immersed with 70 % ethanol. The heating reflux extraction method was employed for the medicinal materials, requiring three rounds of extraction, with the ratios of medicinal materials to 70 % ethanol at 1:15, 1:10 and 1:10, respectively [27]. Subsequently, the extraction solutions were filtered, combined, and concentrated to obtain the *Oroxylum indicum* (L.) Kurz extract with a concentration equivalent to 2.5 g/mL of the raw *Oroxylum indicum* (L.) Kurz material [28,29]. The concentration of oroxin A, oroxin B, baicalin, chrysin, baicalein, scutellarein, apigenin, quercetin, oroxylin A and isorhamnetin were determined to be 12265, 13927, 507.09, 343.65, 378.03, 299.72, 401.92, 231.15, 312.62 and 593.14 ng/mL.

### 2.4. Animals and drug administration

Thirty-six male Sprague-Dawley (SD) rats weighing 200–230 g were procured from Hebei Medical University (Shijiazhuang, China). The rats were acclimated to standard temperature, humidity, and light conditions for 7 days before the experiment. Prior to the experiments, the animals underwent a fasting period of 12 h. The thirty-six rats were randomly assigned into six groups, containing experimental blood (24 h), urine and feces (72 h), and bile groups (24 h) as well as blank blood (24 h), urine and feces (72 h), and bile groups (24 h) [30,31]. All animal procedures adhered to the guideline set by the Research Ethics Committee of the Second Hospital of Hebei Medical University with Ethical Approval No. 2023-AE312. Institutional protocols and ethics were strictly followed throughout all in animal experiments.

### 2.5. Samples collection for metabolic study

#### 2.5.1. Plasma samples

Blood samples were collected from the eye canthus of six rats at 0.17, 0.50, 0.75, 1, 2, 4, 6, 9, 12 and 24 h after administration. Following centrifugation at a speed of 1400g for 5 min (Hunan Xiangyi Laboratory Instrument Development Co. Ltd., Hunan, China), the supernatant was carefully retrieved and all plasma samples were pooled together. Blank plasma was obtained using the same procedure from rats (n = 6) treat with water.

#### 2.5.2. Urine and feces samples

Urine and feces samples were collected at the following time intervals: 0–4 h, 4–8 h, 8–12 h, 12–24 h, 24–36 h, 36–48 h, 48–60 h, and 60–72 h after administrating of the extract. All urine and feces samples were pooled together. The control urine and feces samples were collected using the same method after administrating of water.

#### 2.5.3. Bile samples

The rats were administered a urethane physiological saline solution (1.5–2 g/kg) via gavage, followed by bile duct cannulation. Subsequently, bile samples were collected at 0–1 h, 1–3 h, 3–5 h, 5–8 h, 8–12 h and 12–24 h time intervals. Finally, all the collected bile samples were consolidated. Blank bile samples were obtained from rats subjected to oral water administration.

**Table 1**  
HPLC-ESI-MS/MS data of ten components from *Commelina communis* Linn.

Component	Relative molecular mass	$t_R$ /min	Ion source model	$MS_1(m/z)$	$MS_2(m/z)$	DP/V	CE/eV
Oroxin A	432.4	3.35	ESI <sup>+</sup>	431.3	269.1	−70	−24
Oroxin B	594.5	2.54	ESI <sup>+</sup>	593.4	268.9	−70	−33
Baicalin	446.4	3.74	ESI <sup>+</sup>	445.4	268.7	−80	−50
Chrysin	254.2	7.41	ESI <sup>+</sup>	253.0	143.0	−40	−39
Baicalin	270.2	6.03	ESI <sup>+</sup>	269.2	223.2	−50	−34
Scutellarein	286.2	3.72	ESI <sup>+</sup>	285.2	139.0	−50	−46
Apigenin	270.2	5.25	ESI <sup>+</sup>	268.8	117.1	−60	−53
Quercetin	302.2	4.45	ESI <sup>+</sup>	300.6	116.9	−80	−41
Oroxylin A	284.2	7.74	ESI <sup>+</sup>	283.1	151.0	−40	−26
Isorhamnetin	316.3	5.66	ESI <sup>+</sup>	315.1	267.9	−48	−31
IS	253.3	4.23	ESI <sup>+</sup>	252.2	300.0	−24	−22

## 2.6. Sample pre-treatment

Methanol (10 mL) was added into blood, urine, and bile samples (2 mL), followed by concentration of the supernatants under reduced pressure at 25 °C using a Heidolph Laborota 4001 rotary evaporator (Heidolph Instruments GmbH & Co., Schwabach, Germany). Concentrated samples were dissolved in methanol (200 µL) for further analysis by UHPLC-Q-TOF-MS/MS.

The feces sample (2.0 g) was sonicated with methanol (20 mL) for 45 min. After centrifuging at 10,000g for 10 min, the supernatant was dried under a nitrogen atmosphere. The residue was dissolved in methanol (400 µL).

## 2.7. Preparation of calibration standards and quality control (QC) samples

The stock solutions of oroxin A, oroxin B, baicalin, chrysin, baicalein, scutellarein, apigenin, quercetin, oroxylin A and isorhamnetin were individually weighted and dissolved in methanol. The concentrations of each reference solution were 1.31 mg/mL for oroxin A, 1.24 mg/mL for oroxin B, 1.14 mg/mL for baicalin, 1.08 mg/mL for chrysin, 1.16 mg/mL for baicalein, 1.05 mg/mL for scutellarein, 1.19 mg/mL for apigenin, 1.15 mg/mL for quercetin, 1.04 mg/mL for oroxylin A and 0.88 mg/mL for isorhamnetin. The mixed standard solution for the PK study was prepared by combining ten stock solutions. The concentrations of ten stock solution are list in Table 2. The sulfamethoxazole (IS) standard solution was prepared by dissolving a specified amount in methanol to achieve a concentration of 1.08 µg/mL.

The calibration standards for the ten active compounds were as follows: A 20 µL series of standard solutions and 20 µL internal standard (IS) were added into 100 µL blank plasma, followed by the addition of 500 µL methanol after vortex mixing for 1 min. After vortex mixing for 5 min, the mixture was centrifuged at 12,000g for 10 min. The supernatant was subsequently evaporated under nitrogen gas. Finally, the residue was re-dissolved in 100 µL methanol and centrifuged at 12,000g for another 10 min. The final plasma concentrations and the QC samples prepared with low, medium, and high concentration of ten analytes are list in Table 2.

## 2.8. Preparation of plasma samples for PK study

Protein precipitation was employed for the treatment of all rat plasma samples. A volume of 20 µL internal standard and 20 µL methanol (corresponding to the working solution for the calibration curve and QC sample) were added to each plasma samples (100 µL), followed by vortexing for 5 min. Subsequently, 500 µL methanol was added to denature protein in the mixture, which was then vortexed again for another 5 min before being centrifuged at a speed of 12,000g for 10 min. The resulting supernatant was dried under nitrogen gas at room temperature and reconstituted with 100 µL methanol.

## 2.9. Pharmacokinetic study in rat plasma

A total of sixteen rats were randomly allocated into two groups, with eight rats in each group. Rats in administration group I received *Oroxylum indicum* (L.) Kurz extract, while rats in blank group II were administered with water via intragastric injection. The dose of administration was 15 mL/kg. Blood samples were respectively collected from the inner canthus at specific time point at 0, 5, 10, 15, 25, 60, 90, 180, 360, 720, 1140, and 1800 min after administrating *Oroxylum indicum* (L.) Kurz extract and water. Following centrifugation at a speed of 1800g for 5 min, the plasma layer was stored at -80 °C until further analysis.

The pharmacokinetic parameters of ten analytes were determined using a non-compartment model with DAS software version 3.0 (Beijing, China) [32–36].

## 3. Results and discussion

### 3.1. MSOP theory and methodology

The LC-MS data has been obtained from after sample detection and was imported into Peakview software to extract the retention

**Table 2**

The concentrations of stock solution, final plasma for calibration, and QC sample with low, medium and high of ten analytes.

Compounds concentration (ng/mL)	Standards in stock solution	Final plasma concentration range	QC sample		
			Low	Medium	High
Oroxin A	5894.93	1.26–3894.93	2.52	1921.22	3115.94
Oroxin B	6410.28	1.12–4103.28	2.24	1932.56	3282.62
Baicalin	1084.12	1.35–218.28	2.70	108.72	174.62
Chrysin	980.34	1.25–145.25	2.50	73.98	116.20
Baicalein	720.65	1.44–172.31	2.88	84.45	137.85
Scutellarein	740.22	1.22–126.42	2.44	62.75	101.14
Apigenin	650.12	1.02–198.34	2.04	98.66	158.67
Quercetin	560.46	1.19–67.32	2.38	33.06	53.86
Oroxylin A	436.06	1.32–105.25	2.64	51.96	84.20
Isorhamnetin	420.12	1.03–153.32	2.06	76.14	122.66

time and secondary MS information of all components. Subsequently, an Excel-based two-dimensional matrix was established with retention time (Rt) and mass-to-charge ratio ( $m/z$ ) as column indexes in Excel software. The matrix had a total of  $a$  rows and  $b$  columns, representing  $a \times b$  dimensions. Each row corresponded the MS information of chromatographic components at specific retention time (Rt), while each column represented the chromatographic information of fragment ions with  $m/z$  values. *Oroxylum indicum* (L.) Kurz extract samples were denoted as  $H_{0a \times b}$ , whereas biological samples after administration were labeled as  $H_{a \times b}$ . Herein, “m” represented all medicinal components in the sample, while “e” denoted all metabolites in the sample. Since *Oroxylum indicum* (L.) Kurz extract solely contained medicinal components, whereas administered biological samples contained medicinal components as well as metabolites, Then,

$$H_0 = H_{0m} \quad (\text{Eq. 1})$$

$$H = H_m + H_e \quad (\text{Eq. 2})$$

Among Eq. (1) and Eq. (2),  $H_{0m}$  and  $H_m$  contained the same medicinal components, but they might have different concentrations. The establishment of the orthogonal projection method of mass spectral signals must meet three preconditions: (1) Chromatographic reproducibility, wherein all chromatographic response components retained their retention times under fixed operating conditions; (2) Consistency in data pre-processing, where all samples underwent identical pre-processing procedures; (3) Orthogonality of mass spectral signals implied that the same components exhibit distinct mass spectral characteristics, while different components possessed unique mass spectral features. Although there might be a few identical secondary fragment ions in the mass spectral signal of different components, most of these secondary fragment ions differ between the two component's mass spectral information. Therefore it will be approximated that the mass spectral signals of different components were mutually orthogonal.

Construct of the orthogonal projection matrix  $S_j$  from the mass spectrum vector  $H_{0j}$  of the  $j$  row in the  $H_0$  matrix as follows:

$$S_j = I - (H_{0j})^+ \times (H_{0j}) \quad (j = 1, 2, 3, \dots, a) \quad (\text{Eq. 3})$$

Among Eq. (3),  $I$  was the identity matrix, and “+” was the pseudo-inverse matrix.

Project the dosing biological sample matrix  $H$  with the orthogonal projection matrix  $S_j$ , namely:

$$H_{re} = H \times S_j \quad (j = 1, 2, 3, \dots, a) \quad (\text{Eq. 4})$$

In Eq. (4),  $H_{re}$  was the residual matrix of  $H$ . After the projection, the same mass spectral information as  $H_{0j}$  in the projected matrix  $H$  was eliminated.  $H_{re}$  was the signal matrix after  $H$  eliminating the medicinal material component represented by  $H_{0j}$ .

Take the residual matrix  $H_{re}$  as the new dosing biological sample matrix, namely  $H$  (Eq. (5)):

$$H = H_{re} \quad (j = 1, 2, 3, \dots, a) \quad (\text{Eq. 5})$$

Calculate the next projection matrix  $S_{j+1}$  and residual matrix  $H_{re+1}$  according to Eq. (3) and Eq. (4). Subsequently, another medicinal ingredient was eliminated. In this way, it was repeated a time according to Eq. (3), Eq. (4) and Eq. (5). That was to say, after all a chromatographic components in the *Oroxylum indicum* (L.) Kurz extract sample  $H_0$  were projected to  $H$ , the residual signal matrix  $H_{re}$  only contained the signal of components different from those of the *Oroxylum indicum* (L.) Kurz extract sample  $H_0$ . Then the final signal expressed in the  $H_{re}$  matrix was the signal of the metabolites, namely  $H_e$  (Eq. (6)),

$$H_e = H_{re} \quad (\text{Eq. 6})$$

However, each sample had a baseline signal in addition to the component signal. In order to make the chromatographic baseline area not involved in the projection, this study would do a correlation analysis between the component signal and baseline signal and set a correlation coefficient  $R_j$  as the restriction condition of the projection, namely (Eq. (7)),

$$R_j = \text{corr}(H_{0j}, H_j) \quad (\text{Eq. 7})$$

“Corr” was the correlation calculation of the two vectors, and  $H_{0j}$  and  $H_j$  were respectively *Oroxylum indicum* (L.) Kurz extract sample matrix  $H_0$  and the  $j$ th mass spectral vector signals of the administered biological sample matrix  $H$ . In the analysis of metabolite, the concentrations of the same medicinal component in the *Oroxylum indicum* (L.) Kurz extract sample and the administered biological sample may be different, which would lead to some differences in the chromatographic peaks. There were three possibilities for the two mass spectral vector signal  $H_j$  and  $H_{0j}$ : (1)  $H_j$  and  $H_{0j}$  were both baseline mass spectral vector. (2) One of  $H_j$  and  $H_{0j}$  was the baseline mass spectrum vector, and the other signal was the mass spectrum vector of the plant material components. (3)  $H_j$  and  $H_{0j}$  were both mass spectral vectors of the same medicinal material components. The baseline was caused by noise, and the correlation between noise and noise and between noise and component signals were extremely small. Therefore, only when the value of  $R_j$  was very large indicating that it was the mass spectrum vector of the same plant material component, this cycle could be carried out. On the contrary, it belonged to the first two. The next projection matrix would be directly carried out. It was believed that it was sufficient as long as the correlation coefficient  $R_j$  was above 0.9 by consulting relevant literature and subsequent verification experiments of the MSOP method [35].

### 3.2. MSOP method validation

The study selected four controlled substances including oroxin A, oroxin B, baicalein and oroxylin A. Methanol was used to prepare

mixed samples of A, B and C. Sample A included SA and SC as components of plant material extracts. Sample C included four reference substances (SA, SC, SB<sub>3</sub>, SD) taken as biological samples for drug administration. The concentrations of the corresponding substances in sample A differed from those in SA and SC. Thus, the concentrations of plant materials in administered biological samples were different from those in plant materials samples, which was consistent with the actual metabolite studies. SB<sub>3</sub> and SD were two metabolite components. At the same time, in order to verify whether the signal of metabolites in the biological samples obtained by MSOP method was accurate, a test sample called B sample was designed to include SB<sub>3</sub> and SD. Whether the Chinese medicinal materials SA and SC of sample C could be effectively removed by MSOP method, and the determination of chromatographic conditions of sample UHPLC-MS was based on the following: the chromatographic peaks of SA, SC, SB<sub>3</sub> and SD should be completely separated as far as possible. The original total ion flow chromatograms obtained through UHPLC-MS detection for drug sample A, administered biological sample C, and test sample B are shown in Fig. 1. Based on the MSOP method, the orthogonal projection matrix established by the crude drug sample A was used to deliver the biological sample C. The final calculated chromatographic peak of metabolites and that of actual sample B are shown in Fig. 2. It can be seen from the figure that (1) the chromatographic peaks calculated by MSOP for SB<sub>3</sub> and SD overlapped with their actual chromatographic peaks in test sample B. The chromatographic peaks of components SB<sub>3</sub> and SD were slightly lower than the actual peaks because the concentrations formulated during solution preparation were different, which was consistent with the actual metabolites study. (2) There was no unknown peak in the chromatogram of metabolites obtained from the administered biological sample C calculated by MSOP method, which proved that MSOP method could accurately obtain metabolites. Therefore, MSOP method can be effectively used to eliminate components of Chinese medicinal materials in the study of metabolites.

### 3.3. Analytical strategy and metabolite analysis

The raw data were imported into Peakview software for analysis. Non-target search was performed, and data preprocessing such as peak intensity was set to obtain retention time (Rt) and mass-to charge ( $m/z$ ). Dimensional matrix was established in Excel with retention time (Rt) and mass-to-charge ratio ( $m/z$ ) as row and column indicators. Subsequently, these matrices were imported into Matlab for correlation analysis, resulting in the construction of a projection matrix. The projection matrix of the drug delivery biological sample was carried out to eliminate the same information in the drug delivery biological sample matrix as the sample matrix of plant materials, and the matrix with only metabolite information was obtained. Finally, according to the established database (flavonoid components and fragmentation pattern of metabolites, liquid chromatography retention time, molecular weight and structural information), the metabolites could be effectively searched by comparing the data of the blank sample via Peakview. The structure of the compound was determined by comparing and analyzing the fragmentation pattern of secondary mass spectrometry in the database. Isomers were distinguished from the Clog P value of the compound, in that the higher the Clog P value of the compound, the longer the retention time.

### 3.4. The mass fragmentation of oroxin A, oroxin B, baicalin and baicalein

Oroxin A, oroxin B, baicalin and baicalein had the respective elution time of 14.45, 11.61, 14.18 and 19.49 min, with the respective deprotonated ions at  $m/z$  431.0938, 593.1537, 445.0763 and 269.0453. Oroxin A displayed the secondary fragment ions at  $m/z$  269.0398 [ $M-C_6H_{10}O_5-H$ ]<sup>-</sup>. Oroxin B owed the main fragment ions at  $m/z$  431.1461 [ $M-C_6H_{10}O_5-H$ ]<sup>-</sup> and 269.0081 [ $M-C_{12}H_{20}O_{10}-H$ ]<sup>-</sup>. Baicalin presented the typical product ion at  $m/z$  269.1623 [ $M-C_6H_8O_6-H$ ]<sup>-</sup>. Baicalein had the characteristic product ions at  $m/z$  253.0192 [ $M-O-H$ ]<sup>-</sup> and 241.0154 [ $M-CO-H$ ]<sup>-</sup>. The four main chemical signals of oroxin A, oroxin B, baicalin and baicalein were present in the Chinese medicinal material *Oroxylum indicum* (L.) Kurz, could be converted into each other *in vivo*. Oroxin A result from the loss of  $C_6H_{10}O_5$  based on Oroxin B. Baicalein could be produced from oroxin B losing  $C_{12}H_{20}O_{10}$ , oroxin A losing  $C_6H_{10}O_5$ , baicalin losing  $C_6H_8O_6$ . The four main chemical constituents from mutual transformations were displayed in Fig. 3.

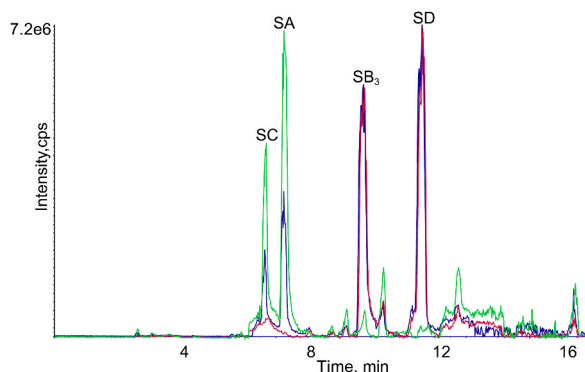
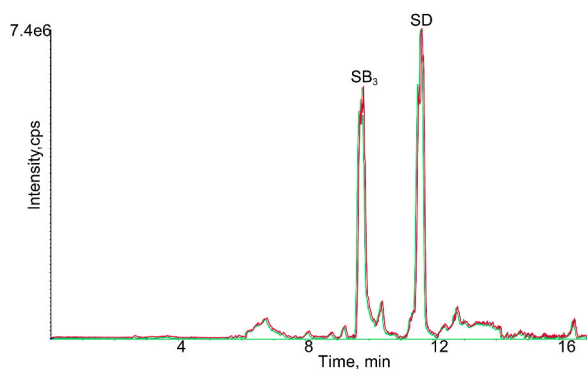
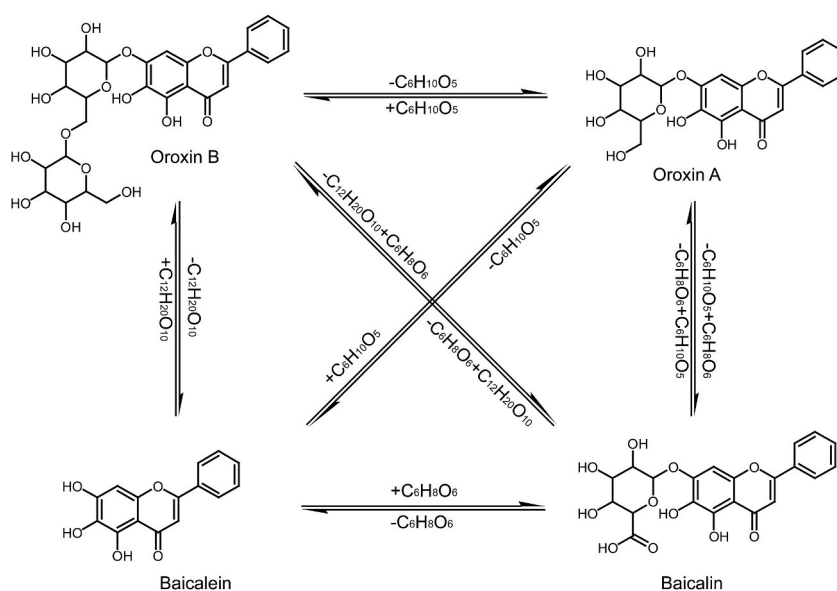


Fig. 1. The total ion chromatograms of sample A, sample B and sample C. (green line: sample A; red line: sample B; blue line: sample C).



**Fig. 2.** The total ion chromatograms of sample B and sample C. (pink red: sample B; green line: the calculated metabolites of sample C using MSOP method).



**Fig. 3.** The four main chemical composition mutual transformations.

### 3.5. Identification of phase I metabolites *in vivo*

A total of 47 metabolites were detected *in vivo*. The detected metabolites are respectively listed in Table 3 with their structures shown in Fig. 4. Their XICs (extracted ion chromatogram) are presented in Fig. 5.

#### 3.5.1. Oxidation reaction

Metabolites M1 and M2 were eluted at 4.94 min and 5.98 min with the deprotonated molecular ions  $[M - H]^-$  was at  $m/z$  477.0581 and  $m/z$  477.0584, respectively. The typical fragment ions at  $m/z$  461.1717 and 445.0563 were found at MS/MS of metabolites, which suggested that the molecular formula of M1 and M2 is  $C_{21}H_{18}O_{13}$ . Moreover, the Clog P values of M1 and M2 were  $-0.860961$  and  $-0.49096$ , respectively.

M3 had a deprotonated molecule ion  $[M - H]^-$  at  $m/z$  463.0882, 32 Da more than that of oroxin A, which indicated that M3 was oxidation metabolite of oroxin A. In addition, M3 was eluted at 10.28 min under the experimental conditions. The classic product ion at  $m/z$  431.1893 was due to a loss of elemental oxygen. The chemical formula of M8 was founded to be  $C_{21}H_{20}O_{12}$ .

Metabolites M4, M5 and M6 showed the respective elution time of 10.54 min, 11.83 min and 12.54 min with respective deprotonated molecular ions  $[M - H]^-$  at  $m/z$  461.0726, 461.0729 and 461.0729. The typical fragment ion at  $m/z$  445.0736 was detected, which suggests that oxidation reaction occurred on the basis of parent drug baicalin. Reaction occurred on the basis of parent drug baicalin. The formula of M4-M6 is  $C_{21}H_{18}O_{12}$  on the basis of the mass data. Moreover, the Clog P values of M4-M6 were  $-0.194819$ ,  $0.105181$  and  $0.105181$  respectively according to ChemDraw (12.0). Therefore, M4-M6 have been characterized based on this data.

Metabolites M7, M8, M9 that eluted at 12.85, 16.92 and 17.52 min showed deprotonated molecular ions  $[M - H]^-$  at  $m/z$  447.0933,

**Table 3**

Summary of phase I and phase II metabolites of main flavonoids in rat blood, urine, bile and feces.

Metabolites ID	Composition shift	Formula	<i>m/z</i>	Error (ppm)	<i>t<sub>R</sub></i> (min)	Score (%)	MS/MS fragments	Clog P	Blood	Urine	Bile	Feces
M1	Oxidation	C <sub>21</sub> H <sub>18</sub> O <sub>13</sub>	477.0581	-1.4	4.94	84.9	461.1717, 445.0563	-0.860961	+ <sup>a</sup>	+	- <sup>b</sup>	-
M2	Oxidation	C <sub>21</sub> H <sub>18</sub> O <sub>13</sub>	477.0584	-1.8	5.98	86.5	461.0550, 445.0492	-0.49096	+ <sup>a</sup>	+	- <sup>b</sup>	-
M3a	Oxidation	C <sub>21</sub> H <sub>20</sub> O <sub>12</sub>	463.0882	-1.1	10.28	83.0	431.1893, 301.1614, 269.2367, 241.0175	-0.382115	-	-	-	+
M3b								-0.0121154				
M4	Oxidation	C <sub>21</sub> H <sub>18</sub> O <sub>12</sub>	461.0726	-1.7	10.54	84.4	445.0736	-0.194819	+	+	-	+
M5	Oxidation	C <sub>21</sub> H <sub>18</sub> O <sub>12</sub>	461.0729	-2.2	11.83	84.6	445.0735	0.105181	+	+	-	+
M6	Oxidation	C <sub>21</sub> H <sub>18</sub> O <sub>12</sub>	461.0729	-2.6	12.54	87.9	445.0738	0.105181	+	+	-	+
M7	Oxidation	C <sub>21</sub> H <sub>20</sub> O <sub>11</sub>	447.0933	-3.1	12.85	87.8	431.0898, 269.4778, 241.0008	0.284027	+	+	-	-
M8	Oxidation	C <sub>21</sub> H <sub>20</sub> O <sub>11</sub>	447.0918	1.5	16.92	88.9	431.1021, 269.0794, 241.1596	0.584027	+	+	-	-
M9	Oxidation	C <sub>21</sub> H <sub>20</sub> O <sub>11</sub>	447.0917	-2.4	17.52	83.6	431.0607, 269.0850, 241.1627	0.584027	+	+	-	-
M10	Oxidation	C <sub>15</sub> H <sub>10</sub> O <sub>7</sub>	301.0354	-1.9	13.27	89.4	285.0421, 269.0742, 241.0975	1.74125	-	+	-	+
M11	Oxidation	C <sub>15</sub> H <sub>10</sub> O <sub>6</sub>	285.0405	-2.8	17.55	88.7	269.2640, 241.2835, 167.2869, 105.0253	2.33739	+	-	-	+
M12a	Oxidation	C <sub>27</sub> H <sub>30</sub> O <sub>17</sub>	625.1410	-1.4	23.39	90.6	609.2907, 593.5824, 431.2891, 301.2903,	2.43136				
M12b							269.2896, 241.2849	-1.95866	-	-	-	+
M13	Loss of O	C <sub>21</sub> H <sub>20</sub> O <sub>9</sub>	415.1035	-1.2	11.92	91.0	253.0721, 225.1226	0.916368	+	+	+	+
M14	Loss of O	C <sub>21</sub> H <sub>20</sub> O <sub>9</sub>	415.1032	-2.2	14.27	84.7	253.3373, 225.1898	2.06637	+	+	+	+
M15	Hydrogenation	C <sub>21</sub> H <sub>20</sub> O <sub>11</sub>	447.0933	1.3	15.16	89.4	271.0372, 243.2034	0.736878	+	+	+	+
M16	Loss of O	C <sub>21</sub> H <sub>22</sub> O <sub>10</sub>	433.1142	0.9	15.64	90.2	271.0372, 243.2034	0.437521	+	+	+	+
M17	Loss of O	C <sub>21</sub> H <sub>22</sub> O <sub>10</sub>	433.1205	1.4	16.70	88.4	271.0362, 243.2066	1.58752	+	+	+	+
M18	Loss of O + Hydrogenation	C <sub>15</sub> H <sub>12</sub> O <sub>4</sub>	255.0663	1.7	16.64	79.3	239.1201, 227.2927	2.72185	+	+	+	+
M19	Loss of O + Hydrogenation	C <sub>15</sub> H <sub>12</sub> O <sub>4</sub>	255.0017	1.5	20.13	83.1	239.5212, 227.2927	3.11185	+	+	+	+
M20	Loss of O + Hydrogenation	C <sub>15</sub> H <sub>12</sub> O <sub>4</sub>	255.2634	-0.5	21.45	88.3	239.4237, 227.0762	3.11185	+	+	+	+
M21	Hydrogenation	C <sub>15</sub> H <sub>12</sub> O <sub>5</sub>	271.0612	-1.6	19.24	79.1	243.2835	2.55023	+	+	-	+
M22a	Loss of O	C <sub>15</sub> H <sub>10</sub> O <sub>4</sub>	253.0506	-1.4	21.51	83.2	225.3052	2.73275	+	+	-	+
M22b								3.56275				
M22c								3.56275				
M23	Oxidation + Sulfate conjugation	C <sub>27</sub> H <sub>30</sub> O <sub>19</sub> S	689.1029	-2.3	6.34	79.6	609.1908, 593.0075, 431.1442, 269.0128	-2.55403	-	-	+	-
M24	Oxidation + Methylation	C <sub>22</sub> H <sub>22</sub> O <sub>13</sub>	493.0988	1.3	7.97	84.8	447.0031, 271.0515	-0.55977	-	+	-	+
M25	Oxidation + Glucuronide conjugation	C <sub>27</sub> H <sub>26</sub> O <sub>18</sub>	637.1077	2.3	8.01	87.2	445.1107, 269.0551	-1.87163	+	+	+	+
M26	Oxidation + Sulfate conjugation	C <sub>21</sub> H <sub>18</sub> O <sub>15</sub> S	541.0294	1.4	9.70	89.4	445.0072, 269.0557	-1.23568	+	+	+	-
M27	Sulfate conjugation	C <sub>27</sub> H <sub>30</sub> O <sub>18</sub> S	673.1115	2.4	10.36	88.5	593.1008, 431.0385, 269.0666, 241.1824	-2.83038	+	+	+	-

(continued on next page)

Table 3 (continued)

Metabolites ID	Composition shift	Formula	<i>m/z</i>	Error (ppm)	<i>t<sub>R</sub></i> (min)	Score (%)	MS/MS fragments	Clog P	Blood	Urine	Bile	Feces
M28	Oxidation + Sulfate conjugation	C <sub>15</sub> H <sub>10</sub> O <sub>9</sub> S	364.9973	-2.4	10.98	86.6	269.1338	0.996524	-	+	-	+
M29	Bis-sulfate conjugation	C <sub>15</sub> H <sub>10</sub> O <sub>11</sub> S <sub>2</sub>	428.9603	-2.3	11.18	84.8	269.1197	-1.06738	+	+	+	-
M30	Glucuronide conjugation	C <sub>27</sub> H <sub>28</sub> O <sub>16</sub>	607.1337	-1.7	11.30	92.8	431.0944, 269.0291	-0.80723	+	+	+	+
M31	Oxidation + Methylation	C <sub>28</sub> H <sub>32</sub> O <sub>16</sub>	623.1618	-2.5	12.41	93.2	593.2055, 269.0455	-0.968035	+	-	-	+
M32	Oxidation + Methylation	C <sub>28</sub> H <sub>32</sub> O <sub>16</sub>	623.1614	-1.6	13.18	90.2	593.2128, 269.0977	-0.408035	+	-	-	+
M33	Sulfate conjugation	C <sub>21</sub> H <sub>18</sub> O <sub>14</sub> S	525.0344	1.5	14.10	83.2	445.0412, 269.0872	-1.73268	+	+	+	+
M34	Sulfate conjugation	C <sub>21</sub> H <sub>20</sub> O <sub>13</sub> S	511.0552	-0.8	14.11	84.5	431.0612, 269.0873	-1.25383	+	+	+	+
M35	Oxidation + Methylation	C <sub>22</sub> H <sub>20</sub> O <sub>12</sub>	475.0882	-1.2	15.11	84.1	445.1156, 269.0189	0.689666	+	+	-	+
M36a	Glycine conjugation	C <sub>17</sub> H <sub>13</sub> O <sub>6</sub> N	326.0671	-1.4	15.75	81.2	308.0254, 282.1285, 269.1172, 264.1201	0.914016	+	+	+	+
M36b								1.49402				
M36c								1.74404				
M37	Methylation	C <sub>22</sub> H <sub>20</sub> O <sub>11</sub>	459.0933	-0.7	16.44	88.3	445.2028, 269.0035	0.163319	+	+	+	+
M38	Methylation	C <sub>22</sub> H <sub>20</sub> O <sub>11</sub>	459.0957	-0.9	17.47	78.1	445.0191, 269.2096	0.963319	+	+	+	+
M39	Sulfate conjugation	C <sub>21</sub> H <sub>20</sub> O <sub>14</sub> S	527.0417	-1.8	16.62	75.5	431.2812, 269.0623	-0.977485	+	-	-	-
M40	Oxidation + Methylation	C <sub>22</sub> H <sub>22</sub> O <sub>11</sub>	461.1102	-1.1	17.46	78.9	431.2812, 269.1107	1.16852	-	+	-	+
M41	Sulfate conjugation	C <sub>15</sub> H <sub>10</sub> O <sub>8</sub> S	349.0024	-2.1	18.47	89.3	269.0456	0.604616	+	-	+	+
M42	Sulfate conjugation	C <sub>15</sub> H <sub>10</sub> O <sub>8</sub> S	349.0018	-2.4	19.37	82.4	269.2884	1.43462	+	-	+	+
M43	Methylation	C <sub>22</sub> H <sub>22</sub> O <sub>10</sub>	445.1142	-1.4	18.87	90.4	431.0535, 269.0037	0.64217	+	+	+	+
M44	Oxidation + Methylation	C <sub>16</sub> H <sub>12</sub> O <sub>6</sub>	299.0561	-1.5	19.20	79.7	269.0619	2.36187	+	+	-	+
M45	Oxidation + Methylation	C <sub>16</sub> H <sub>12</sub> O <sub>6</sub>	299.0570	-0.9	19.48	86.3	269.2066	2.92187	+	+	-	+
M46a	Acetylation	C <sub>17</sub> H <sub>12</sub> O <sub>6</sub>	311.0561	-1.8	19.30	79.6	269.0085	1.93062	+	+	+	+
M46b								2.51062				
M46c								2.76062				
M47a	Methylation	C <sub>16</sub> H <sub>12</sub> O <sub>5</sub>	283.0612	-1.6	21.92	85.7	269.0656, 241.0501	2.50062	+	+	+	+
M47b								3.08062				
M47c								3.33062				

c

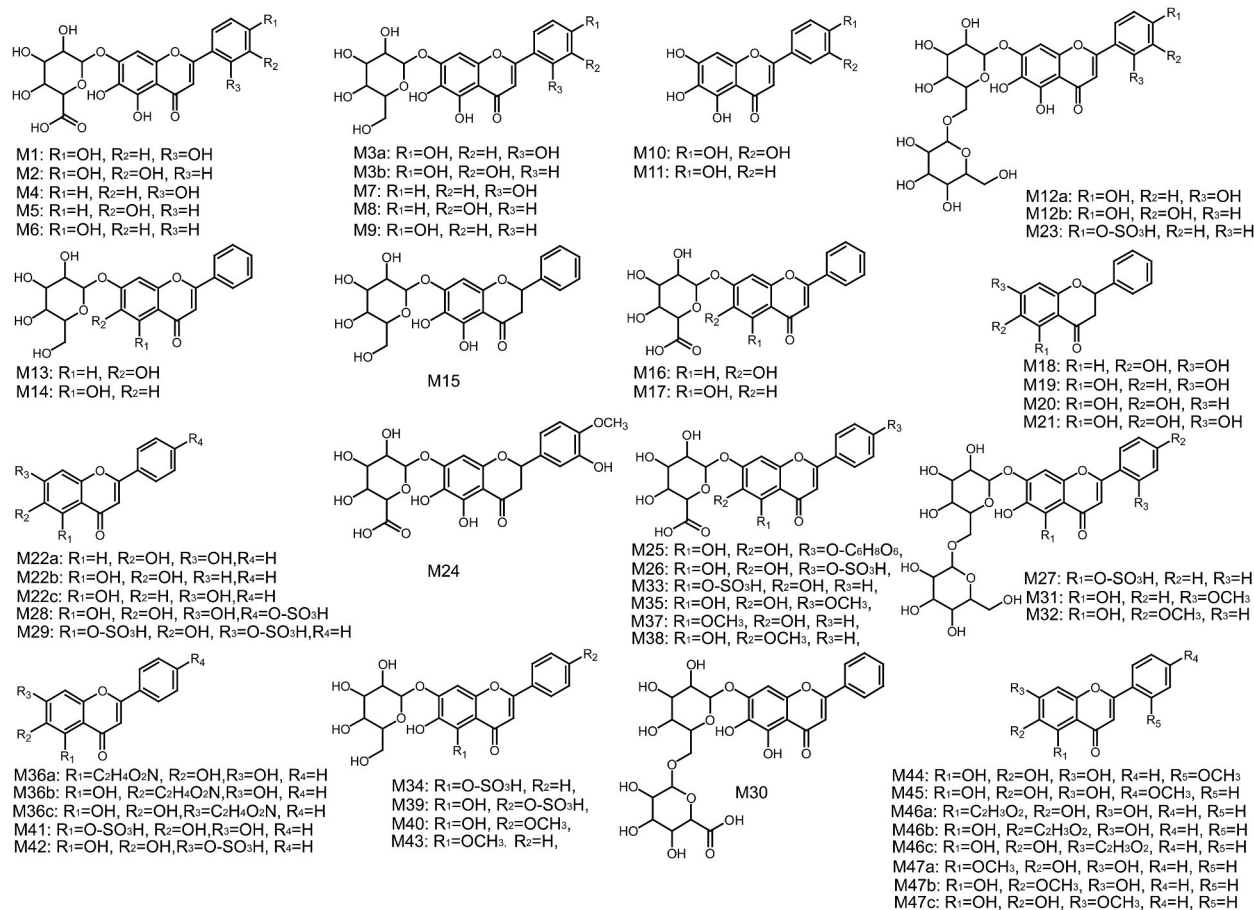


Fig. 4. Chemical structures of all metabolites (R<sub>1</sub>, R<sub>2</sub>, R<sub>3</sub>, R<sub>4</sub> and R<sub>5</sub>, different substituent group).

447.0918 and 447.0917, respectively. The typical fragment ion at  $m/z$  431.0898 was detected suggesting that an oxidation reaction occurred on the basis of baicalin. Thus, the chemical formula for M7-M9 calculated as C<sub>21</sub>H<sub>20</sub>O<sub>11</sub>.

The mass spectrometry analysis of M10 revealed the presence of a deprotonated ion at  $m/z$  301.0354, which was 32 Da higher than that of baicalein. Based on this information, the chemical formula of M10 was determined to be C<sub>15</sub>H<sub>10</sub>O<sub>7</sub>. M11 exhibited a deprotonated ion at  $m/z$  285.0405, which was 16 Da higher than that of baicalein. Additionally, it eluted at a retention time of 17.55 min in the extracted ion chromatogram (XIC). The molecular formula for M11 was inferred as C<sub>15</sub>H<sub>10</sub>O<sub>6</sub>. M12 had an elution time of 23.39 min and afforded a deprotonated ion at  $m/z$  625.1410. The fragment ions at  $m/z$  609.2907 and 593.5824 were generated after loss of O and 2O, respectively, suggesting an oxidation reaction occurred for oroxin B. The molecular formula for M12 was deduced as C<sub>27</sub>H<sub>30</sub>O<sub>17</sub>.

### 3.5.2. Reduction reaction

Two sharp peaks of M13 and M14 were respectively eluted at 11.92 min and 14.27 min with the deprotonated ions at  $m/z$  415.1035 and 415.1032 based on online acquisition, 16 Da less than that of oroxin A. Further, various typical ions at  $m/z$  253.0721 and 225.1226 were formed by the loss of C<sub>6</sub>H<sub>10</sub>O<sub>5</sub> and CO. M13 and M14 had the same chemical formula that was C<sub>21</sub>H<sub>20</sub>O<sub>9</sub>. Moreover, the respective Clog P values showed as 0.916368 and 2.06637.

M15, with the retention time at 12.93 min, had a deprotonated ion at  $m/z$  447.0933, 2 Da higher than the mass of baicalin. The typical fragment ion at  $m/z$  271.0960 was obtained by loss of C<sub>6</sub>H<sub>8</sub>O<sub>6</sub>, which was 2 Da more than that of baicalin losing C<sub>6</sub>H<sub>8</sub>O<sub>6</sub>. The M15 was inferred as C<sub>21</sub>H<sub>20</sub>O<sub>11</sub>. M16 and M17 were extracted at 15.16 and 16.70 min under the UHPLC conditions, and obtained quasi-molecular ion at  $m/z$  433.1142, showing 2 Da increase from oroxin A. The chemical formula of M16 and M17 were found to be C<sub>21</sub>H<sub>22</sub>O<sub>10</sub>.

On the basis of the UHPLC-MS data, M18-M20 gave rise to deprotonated ions at  $m/z$  255.0663, 255.0017 and 255.2634 with respective elution time of 16.64, 20.13 and 21.45 min. M18-M20 showed 14 Da less than that of baicalein and had the same chemical composition of C<sub>15</sub>H<sub>12</sub>O<sub>4</sub>. Some representative ions at  $m/z$  239.1201 and 227.2927 were received via losing O and CO, respectively. The Clog P values of M18-M20 were 2.72185, 3.11185 and 3.11185, calculated by ChemDraw 14.0.

M21 was washed-out at 19.24 min through gradient elution and had the deprotonated ion at  $m/z$  271.0612, 2 Da more than that of baicalein. The characteristic fragment ion at  $m/z$  243.2835 ([M - CO]<sup>-</sup>) revealed the molecular formula for M21 of C<sub>15</sub>H<sub>12</sub>O<sub>5</sub>. M22

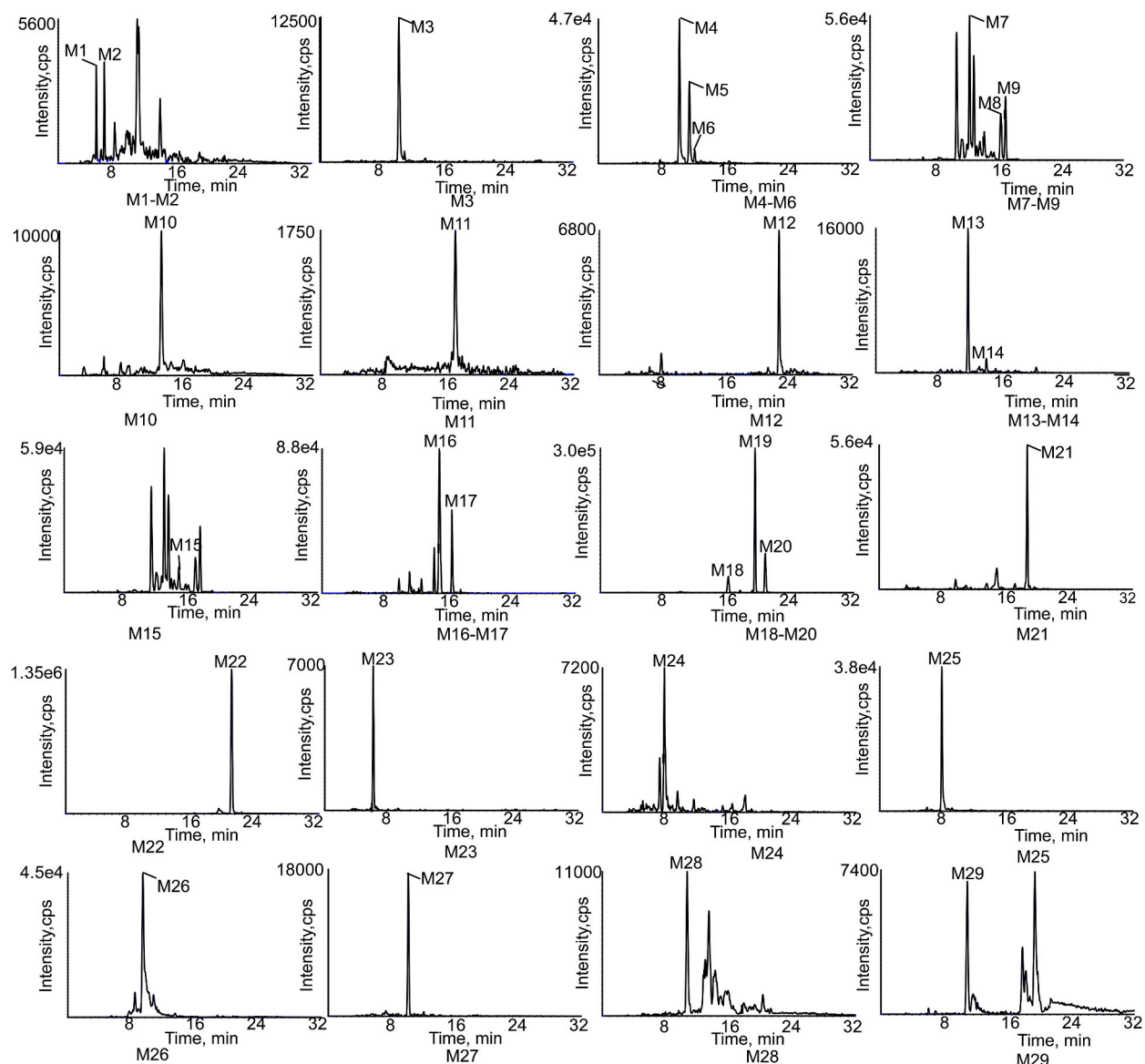


Fig. 5. Extracted ion chromatograms of all metabolites.

eluted at 21.51 min with the deprotonated ion at  $m/z$  253.0506, was 16 Da less than the  $m/z$  of baicalin. The molecular formula of M22 was inferred as  $C_{15}H_{10}O_4$ . The characteristic ion at  $m/z$  225.3052 was revealed by loss of CO. M22 was due to baicalin losing an oxygen molecule.

### 3.6. Identification of phase II metabolites in vivo

M23, eluted at 6.34 min, showed a molecular ion  $[M - H]^-$  at  $m/z$  689.1029 ( $C_{27}H_{30}SO_{19}$ ), which was 96 Da higher than that of oxroin B. In addition, typical fragment ions at  $m/z$  609.1908, 593.0075, 431.1442 and 269.0128 were detected in the mass spectrum, which are due to the respective loss of  $SO_3$ , O,  $C_6H_{10}O_5$  and  $C_6H_{10}O_5$ . M24 had a deprotonated molecule ion  $[M - H]^-$  at  $m/z$  493.0988, 48 Da more than that of baicalin. M24 showed an elution peak at 7.97 min. The product ions at  $m/z$  445.0031 ( $[M-2O-CH_2-H]^-$ ) and 269.0515 ( $[M-2O-CH_2-C_6H_{10}O_5-H]^-$ ) were detected, which revealed that oxidation and methylation reactions occurred. The molecular formula of M24 was deduced as  $C_{22}H_{22}O_{13}$ .

The molecular formula of M25 is  $C_{27}H_{26}O_{18}$  according to the characteristic product ions at  $m/z$  431.1107 ( $[M-O-C_6H_8O_6-H]^-$ ) and 269.0551 ( $[M-O-C_6H_8O_6-C_6H_8O_6-H]^-$ ). M25 showed a deprotonated molecule ion  $[M - H]^-$  at  $m/z$  637.1077 and was eluted at 8.01 min. M26 with deprotonated molecule ions  $[M - H]^-$  at  $m/z$  541.0294 eluted at 9.70 min, which is deduced as an oxidation, a sulfation

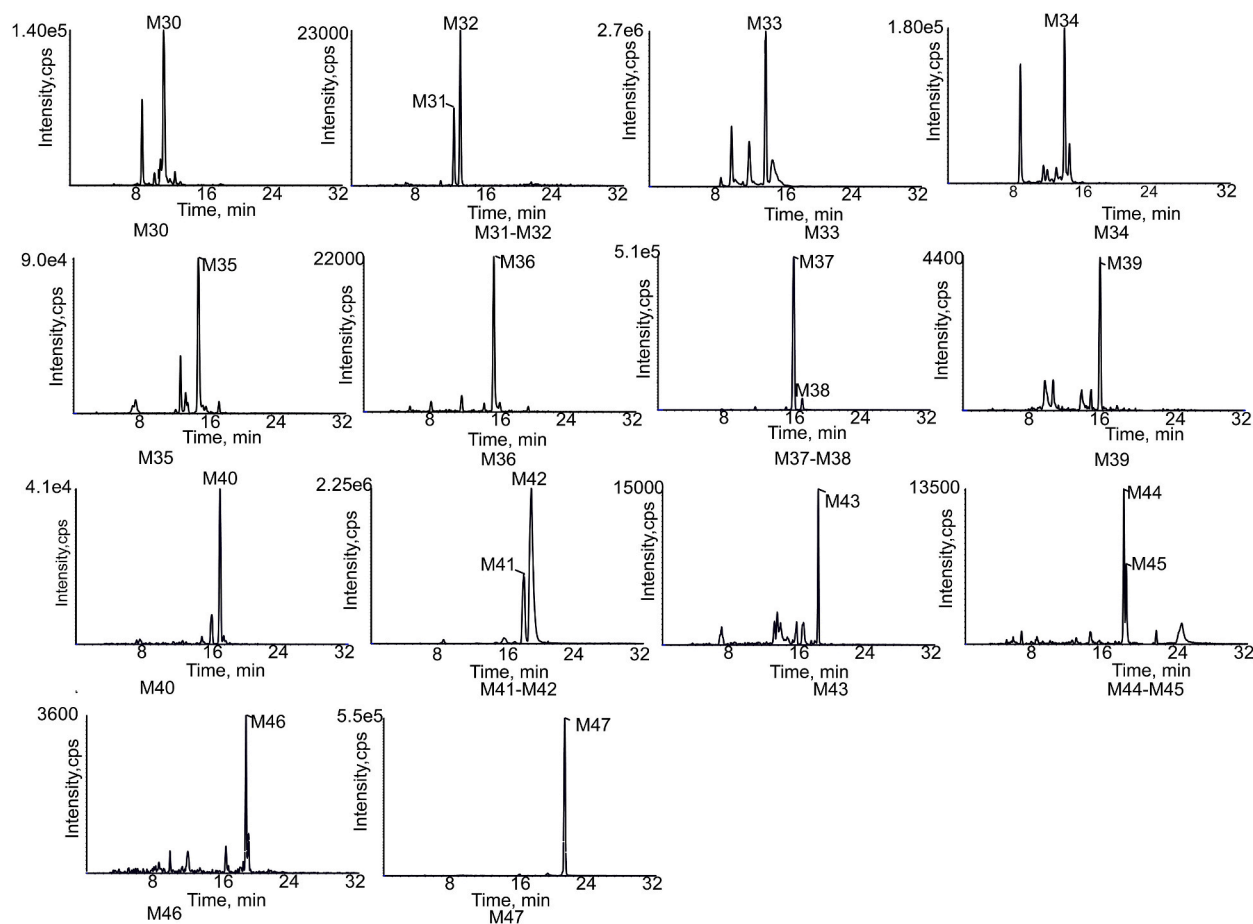


Fig. 5. (continued).

and a glucuronidation reaction of baicalein. The chemical formula is calculated as  $C_{21}H_{18}SO_{15}$ . The secondary fragment ions are at  $m/z$  445.0072 ( $[M-O-SO_3-H]^-$ ) and  $m/z$  269.0557 ( $[M-O-SO_3-C_6H_8O_6-H]^-$ ). M27 exhibited the molecular composition of  $C_{27}H_{30}SO_{18}$ , eluted one sharp peak at 10.36 min, and possessed the deprotonated molecule ions  $[M-H]^-$  at  $m/z$  673.1115. M27 showed a neutral addition of 80 Da ( $SO_3$ ) to oroxin B that suggests a sulfation conjugation reaction of oroxin B.

M28 exhibits a molecular composition of  $C_{15}H_{10}SO_9$  with the deprotonated molecular ions  $[M-H]^-$  at  $m/z$  364.9973, and was eluted at 10.98 min. The fragment ion at  $m/z$  269.1338 was attributed to the consecutive loss of O and  $SO_3$ , which provides sound evidence to characterize the metabolite. Meanwhile, M29 with an elution time at 11.18 min exhibited the deprotonated molecule ions  $[M-H]^-$  at  $m/z$  428.9603, which is 160 Da greater than that of baicalein. Moreover, a key ion at  $m/z$  269.1197 ( $[M-2SO_3-H]^-$ ) was discovered via TOF-MS analysis. M29 was revealed as  $C_{15}H_{10}S_2O_{11}$ . M30 showed a sharp peak at 11.30 min, with the deprotonated molecule ions  $[M-H]^-$  at  $m/z$  607.1337 under the experimental condition, showing 176 Da more than that of oroxin A. The chemical formula of M30 is  $C_{27}H_{28}O_{16}$  that are glucuronide conjugation metabolites of oroxin A.

Two sharp peaks of M31 and M32, whose respective retention times were at 12.41 min and 13.18 min, show quasi-molecular ions  $[M-H]^-$  at  $m/z$  623.1618 and 623.1614, exhibiting 30 Da more than MS/MS of oroxin B. In addition, the elemental composition is  $C_{28}H_{32}O_{16}$ . M31 and M32 were oxidation and methylation metabolites of oroxin B. Some notable ions at  $m/z$  593.2055 and  $m/z$  269.0455 were gained via loss of  $CH_2$ , O and  $C_{12}H_{20}O_{10}$ . The calculated Clog P values are  $-0.968035$  and  $-0.408035$ , respectively. M31 and M32 were identified on the basis of all the findings. M33 that eluted at 14.10 min has a calculated chemical formula of  $C_{21}H_{18}SO_{14}$  showing one quasi-molecular ion at  $m/z$  525.0344, which increased 80 Da from baicalin. In the MS/MS spectrum, productive ions at  $m/z$  445.0412 and 269.0872 were gained by loss of  $SO_3$  and  $C_6H_8O_6$ . The results suggested that a sulfation reaction occurred for baicalin.

M34 showed a sharp peak at 14.11 min and a quasi-molecular ion  $[M-H]^-$  at  $m/z$  511.0552 in the negative ion mode. The elemental composition is  $C_{21}H_{20}SO_{13}$  showing an increased of 80 Da from deprotonated oroxin A. The typical fragment ions at  $m/z$  431.0612 ( $[M-SO_3-H]^-$ ) and 269.0873 ( $[M-SO_3-C_6H_{10}O_5-H]^-$ ) verified the fact that M34 is a sulfation metabolite of oroxin A. M35 showed a retention time at 15.11 min, which revealed a quasi-molecular ion  $[M-H]^-$  at  $m/z$  475.0882, that is 30 Da ( $O + CH_2$ ) greater than the  $m/z$  for baicalin. Moreover, the chemical formula of M35 was assigned as  $C_{22}H_{20}O_{12}$ . The characteristic ions at  $m/z$  445.1156

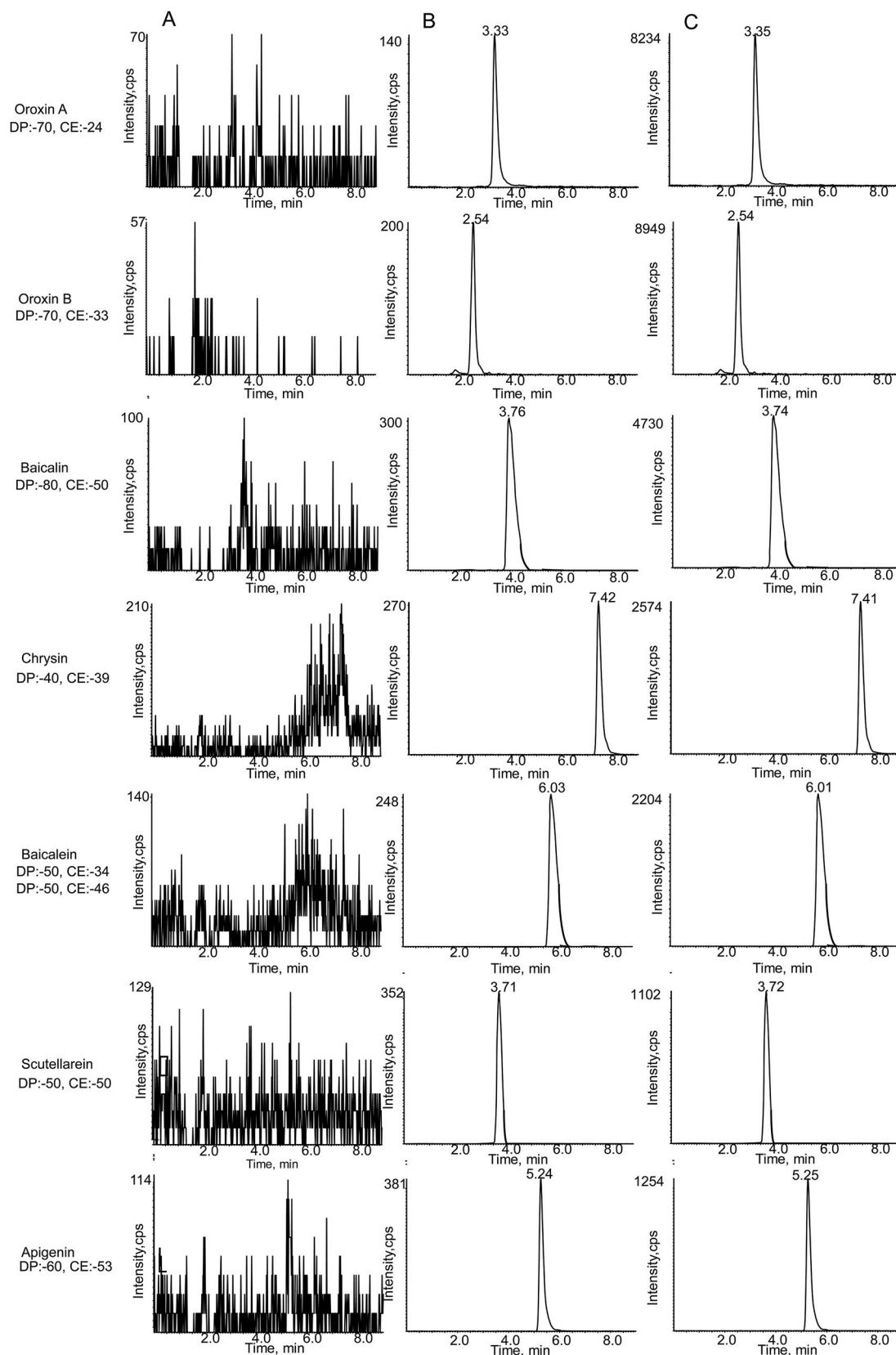


**Fig. 6.** Typical chromatograms of main flavonoids and sulfamethoxazole (IS) in rat plasma: (A) blank plasma; (B) blank plasma spiked with the ten analytes at LLOQ and IS; (C) 15 min sample plasma after a single oral administration of *Oroxyllum indicum* (L.) Kurz extract.

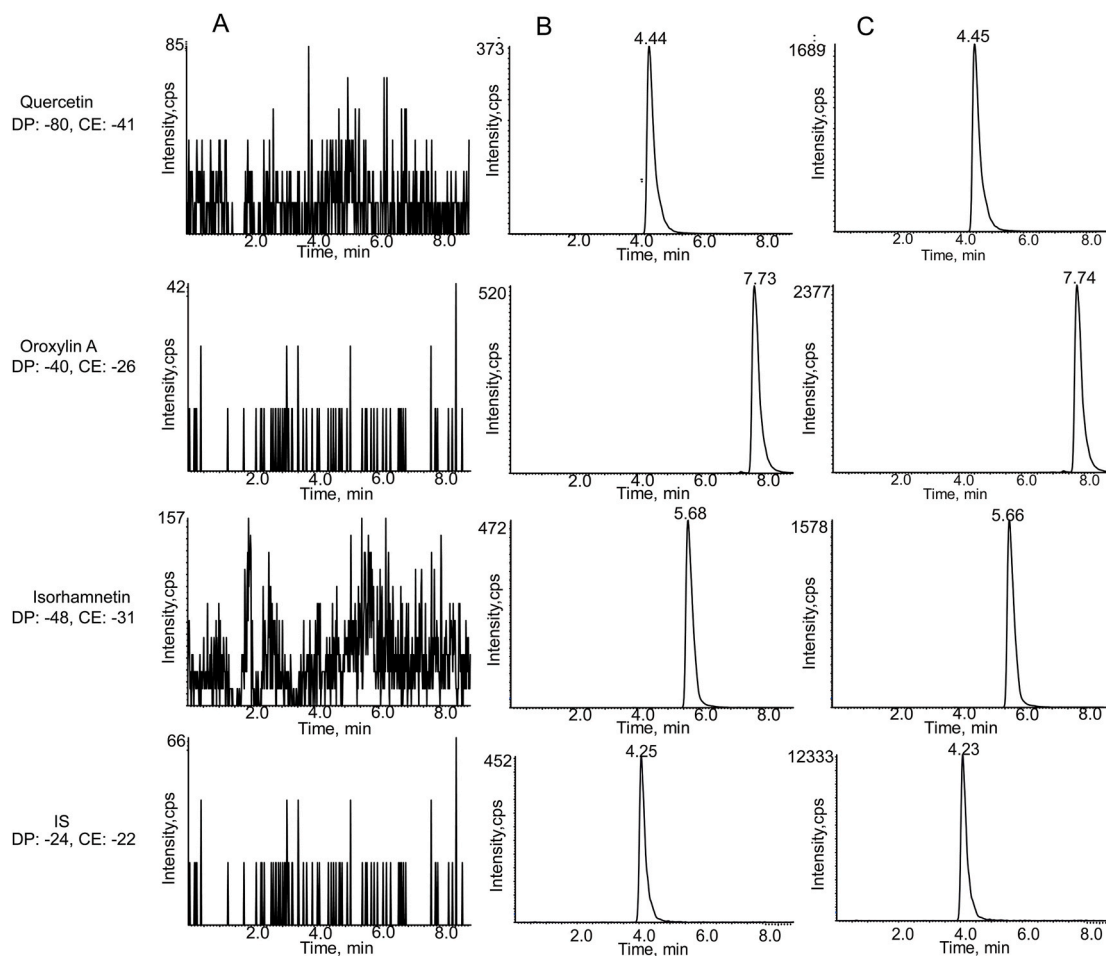


Fig. 6. (continued).

([M-O-CH<sub>2</sub>-H]<sup>-</sup>) and 269.0189 ([M-O-CH<sub>2</sub>-C<sub>6</sub>H<sub>8</sub>O<sub>6</sub>-H]<sup>-</sup>) verified the fact that M35 resulted from the oxidation and methylation reaction. A sharp peak appeared at 15.75 min with the deprotonated ion at  $m/z$  326.0671, 57 Da increasing from baicalin. The second fragment ions at  $m/z$  308.0254, 282.1285 and 264.1201 were obtained from the respective losses of H<sub>2</sub>O, CO<sub>2</sub>, H<sub>2</sub>O + CO<sub>2</sub>. An abundant product ion at  $m/z$  269.1172 resulted from loss of C<sub>2</sub>H<sub>3</sub>NO. The chemical formula of M36 was C<sub>17</sub>H<sub>13</sub>NO<sub>6</sub>. It illustrated that M36 was metabolite of glycine conjugation of baicalin.

M37 and M38 showed elution times at 16.44 and 17.47 min, respectively and exhibited the quasi-molecular ions [M - H]<sup>-</sup> at  $m/z$  459.0933 and 459.0957 showing that it increased by 14 Da from baicalin. Moreover, M37 and M38 possessed the same chemical

Table 4

The regression equations, linear range, LLOQs and LODs of 10 components from *Oroxylum indicum* (L.) Kurz for pharmacokinetic study.

Analyte	Regression equation	R <sup>2</sup>	Linear range (ng/mL)	LLOQ (ng/mL)
Oroxin A	$y = 0.1027x + 0.2721$	0.9979	1.26–3894.93	1.26
Oroxin B	$y = 0.2117x + 0.0065$	0.9985	1.12–4103.28	1.12
Baicalin	$y = 0.1037x + 0.0176$	0.9974	1.35–218.28	1.35
Chrysin	$y = 0.0178x + 0.0089$	0.9983	1.25–145.25	1.25
Baicalin	$y = 0.1003x + 0.0253$	0.9979	1.44–172.31	1.44
Scutellarein	$y = 0.0063x + 0.1027$	0.9991	1.22–126.42	1.22
Apigenin	$y = 0.0094x + 0.0013$	0.9982	1.02–198.34	1.02
Quercetin	$y = 0.2188x + 0.1578$	0.9971	1.19–67.32	1.19
Oroxylin A	$y = 0.0446x + 0.0378$	0.9983	1.32–105.25	1.32
Isorhamnetin	$y = 0.0487x - 0.0073$	0.9969	1.03–153.32	1.03

a) Y, peak area and X, concentration (ng/mL).

b) LOD (S/N = 3).

**Table 5**

The intra-day and inter-day accuracies and precisions of 10 components in rat plasma at low, medium, and high concentration levels (n = 6).

Compounds spiked concentration (ng/mL)	Intra-day (n = 6)			Inter-day (n = 6)		
	Measured concentration (ng/mL)	Accuracy (%)	Precision (%)	Measured concentration (ng/mL)	Accuracy (%)	Precision (%)
Oroxin A						
1.26	1.28 ± 3.38	3.22	5.44	1.33 ± 6.48	4.95	7.88
2.52	2.57 ± 2.38	1.98	4.14	2.62 ± 3.36	3.97	4.53
1921.22	1953.11 ± 4.25	1.66	3.04	1974.82 ± 4.34	2.79	3.58
3115.94	3199.45 ± 4.76	2.68	4.96	3197.58 ± 2.01	2.62	4.46
Oroxin B						
1.12	1.25 ± 4.45	4.03	4.98	1.32 ± 5.28	5.06	6.53
2.24	2.27 ± 5.24	1.34	4.57	2.28 ± 6.19	1.79	3.64
1932.56	1997.88 ± 4.63	3.38	6.23	2007.54 ± 7.42	3.88	7.25
3282.62	3339.08 ± 8.65	1.72	4.01	3362.06 ± 4.89	2.42	5.44
Baicalin						
1.35	1.53 ± 4.26	3.79	5.66	1.59 ± 6.89	4.93	7.48
2.70	2.79 ± 3.04	3.33	5.17	2.78 ± 6.09	2.96	7.83
108.72	112.62 ± 2.36	3.59	6.31	113.48 ± 5.12	4.38	5.03
174.62	179.79 ± 3.53	2.96	4.04	178.72 ± 8.48	2.35	4.99
Chrysin						
1.25	1.42 ± 3.28	5.99	4.09	1.47 ± 7.01	5.01	7.89
2.50	2.64 ± 3.31	5.60	6.85	2.66 ± 7.04	6.40	8.34
73.98	76.07 ± 4.52	2.83	4.16	78.23 ± 6.46	5.74	7.66
116.20	118.02 ± 5.81	1.57	3.58	123.78 ± 8.43	6.52	7.89
Baicalein						
1.44	1.59 ± 5.01	5.22	6.03	1.58 ± 6.24	4.68	7.96
2.88	2.96 ± 4.63	2.78	6.75	3.02 ± 6.44	4.86	6.69
84.45	87.30 ± 3.63	3.37	4.39	89.08 ± 8.66	5.48	6.75
137.85	142.3 ± 5.53	3.23	4.51	141.36 ± 5.18	2.55	5.47
Scutellarein						
1.22	1.43 ± 4.89	3.89	5.97	1.46 ± 7.22	6.86	8.27
2.44	2.48 ± 4.15	1.64	5.48	2.59 ± 7.14	6.15	6.64
62.75	64.75 ± 3.54	3.19	6.46	64.74 ± 4.68	3.17	4.28
101.14	103.52 ± 4.75	2.35	5.17	105.67 ± 6.23	4.48	3.64
Apigenin						
1.02	1.21 ± 4.74	3.65	5.25	1.29 ± 8.02	5.76	7.53
2.04	2.10 ± 6.28	2.94	4.89	2.14 ± 4.96	4.90	4.86
98.66	100.29 ± 7.32	1.65	6.77	103.68 ± 4.59	5.09	5.88
158.67	163.06 ± 3.35	2.77	4.55	165.02 ± 6.52	4.00	5.29
Quercetin						
1.19	1.31 ± 3.99	4.25	5.37	1.37 ± 6.63	4.48	5.83
2.38	2.46 ± 4.84	3.36	5.41	2.49 ± 6.99	4.62	6.93
33.06	33.98 ± 5.88	2.78	6.09	35.49 ± 3.96	7.35	5.73
53.86	55.29 ± 4.42	2.66	4.22	57.27 ± 4.46	6.33	8.04
Oroxylin A						
1.32	1.45 ± 5.32	2.88	4.92	1.52 ± 5.34	5.38	4.29
2.64	2.69 ± 5.58	1.89	6.88	2.78 ± 3.37	5.30	7.42
51.96	53.85 ± 6.75	3.64	4.12	55.02 ± 4.38	5.89	6.38
84.20	86.65 ± 4.38	2.91	3.65	88.08 ± 3.17	4.61	4.64
Isorhamnetin						
1.03	1.15 ± 5.42	3.88	4.04	1.19 ± 4.22	5.94	6.69
2.06	2.15 ± 8.18	4.37	3.58	2.15 ± 8.02	4.37	4.57
76.14	77.85 ± 7.54	2.25	5.22	82.43 ± 9.98	8.26	6.98
122.66	124.29 ± 6.25	1.33	3.95	128.31 ± 5.24	4.61	7.75

formula of  $C_{22}H_{20}O_{11}$ . The characteristic fragment ions at  $m/z$  445.2028 ( $[M-CH_2-H]^+$ ) and 269.0035 ( $[M-CH_2-C_6H_8O_6-H]^+$ ) were detected in the MS/MS of M37 and M38, which suggested that M37 and M38 were methylation metabolites based on baicalin. In addition, the Clog P values of M37 and M38 were 0.163319 and 0.963319, respectively. M37 and M38 were identified on the basis of the Clog P values.

The sharp peak of M39, whose retention time was at 16.62 min, was detected with the deprotonated ion at  $m/z$  527.0417, 96 Da increase from oroxin A. Moreover, the chemical formula of M39 was founded to be  $C_{21}H_{20}SO_{14}$  according to the secondary fragment ions at  $m/z$  431.2812 ( $[M-O-SO_3-H]^+$ ) and 269.0623 ( $[M-O-SO_3-C_6H_{10}O_5-H]^+$ ). M40 exhibited the molecular composition of  $C_{22}H_{22}O_{11}$  and had the elution time at 17.46 min with the deprotonated ion at  $m/z$  461.1102. The typical fragment ions at  $m/z$  431.2812 and 269.1107 were detected by loss of O and  $CH_2$  based on the parent drug oroxin A, which implied that oxidation and methylation reaction happened on the basis of oroxin A. Two deprotonated compounds of M41 and M42 were observed at  $m/z$  349.0024 and 349.0018, respectively, and presented the same chemical formula of  $C_{15}H_{10}SO_8$ . M41 and M42 displayed two individual sharp peaks eluted at 18.47 and 19.37 min, respectively. M41 and M42 went through loss of  $SO_3$ . Moreover, a key ion at  $m/z$  269.0456

**Table 6**  
Stability of ten flavonoids in rat plasma (n = 3).

Compounds spiked concentration (ng/mL)	Short-term stability (room temperature for 8 h)		Long-term stability (-20 °C for 21 d)		Free-thaw stability (3 free thaw cycles)		Post-preparation stability (room temperature for 4 h)	
	Measured concentration <sup>a</sup> (ng/mL)	Accuracy (%)	Measured concentration <sup>a</sup> (ng/mL)	Accuracy (%)	Measured concentration <sup>a</sup> (ng/mL)	Accuracy (%)	Measured concentration <sup>a</sup> (ng/mL)	Accuracy (%)
Oroxin A								
2.52	2.61 ± 7.67	3.57	2.64 ± 18.85	4.65	2.66 ± 6.37	5.63	2.71 ± 6.31	7.47
1921.22	2029.38 ± 9.73	5.63	1996.92 ± 17.92	3.94	2042.64 ± 13.54	6.32	2081.64 ± 6.77	8.35
3115.94	3253.98 ± 16.78	4.43	3297.91 ± 25.15	5.84	3350.57 ± 15.68	7.53	3314.43 ± 15.29	6.37
Oroxin B								
2.24	2.33 ± 8.81	4.02	2.38 ± 8.26	6.37	2.39 ± 13.85	6.48	2.41 ± 4.08	7.47
1932.56	2024.55 ± 9.41	4.76	2021.65 ± 9.48	4.61	2042.33 ± 8.24	5.68	2066.68 ± 12.33	6.94
3282.62	3478.92 ± 20.51	5.98	3400.14 ± 21.74	3.58	3530.46 ± 13.36	7.55	3520.61 ± 14.88	7.25
Baicalin								
2.70	2.83 ± 0.98	4.81	2.87 ± 7.86	6.35	2.87 ± 5.63	6.43	2.94 ± 5.16	8.85
108.72	115.09 ± 4.92	5.86	114.41 ± 9.36	5.23	115.47 ± 6.48	6.21	116.78 ± 3.07	7.41
174.62	185.52 ± 5.49	6.24	184.10 ± 14.47	5.43	187.51 ± 14.57	7.38	189.22 ± 2.75	8.36
Chrysin								
2.50	2.63 ± 4.25	5.20	2.65 ± 10.32	6.03	2.66 ± 1.89	6.37	2.74 ± 0.32	9.79
73.98	77.32 ± 3.22	4.51	76.52 ± 12.94	3.43	79.35 ± 6.99	7.26	78.74 ± 4.17	6.44
116.20	124.19 ± 9.47	6.88	123.20 ± 16.28	6.02	122.97 ± 5.36	5.83	124.26 ± 5.48	6.94
Baicalein								
2.88	3.02 ± 5.94	4.86	3.09 ± 7.51	7.14	3.10 ± 10.25	7.67	3.07 ± 1.76	6.53
84.45	89.82 ± 4.47	6.36	89.08 ± 10.02	5.48	91.74 ± 5.83	8.63	91.09 ± 7.43	7.86
137.85	145.39 ± 6.35	5.47	146.82 ± 18.49	6.51	150.96 ± 13.84	9.51	147.20 ± 9.43	6.78
Scutellarein								
2.44	2.53 ± 2.36	3.69	2.56 ± 6.27	5.11	2.57 ± 3.28	5.14	2.57 ± 8.16	5.46
62.75	66.05 ± 6.34	5.26	66.75 ± 6.21	6.38	66.63 ± 4.36	6.18	66.60 ± 9.46	6.13
101.14	105.37 ± 4.88	4.18	105.83 ± 11.55	4.64	108.43 ± 15.37	7.21	108.26 ± 12.65	7.04
Apigenin								
2.04	2.13	4.41	2.19	7.22	2.18	6.64	2.18	6.94
98.66	102.27	3.66	104.56	5.98	104.34	5.76	103.28	4.68
158.67	167.75	5.72	168.81	6.39	171.40	8.02	171.41	8.03
Quercetin								
2.38	2.47	3.78	2.52	5.84	2.52	5.77	2.55	6.94
33.06	34.48	4.30	34.47	4.28	35.49	7.35	35.55	7.53
53.86	57.54	6.83	57.44	6.64	57.61	6.96	58.40	8.42
Oroxylin A								
2.64	2.79	5.68	2.85	7.92	2.89	9.36	2.84	7.44
51.96	55.29	6.41	56.23	8.22	56.41	8.57	56.61	8.95
84.20	87.75	4.21	89.87	6.73	92.01	9.27	90.41	7.38
Isorhamnetin								
2.06	2.17 ± 0.13	5.34	2.20 ± 0.12	6.97	2.23 ± 0.14	8.45	2.19 ± 0.35	6.45
76.14	81.15 ± 2.92	6.58	80.41 ± 9.44	5.61	82.17 ± 4.54	7.92	79.90 ± 4.56	4.94
122.66	131.32 ± 11.92	7.06	132.40 ± 18.52	7.94	129.05 ± 11.91	5.21	133.16 ± 9.32	8.56

was observed using TOF-MS analyzer. Since the Clog P values of M40 and M41 were 0.604616 and 1.43462, respectively.

M43 eluted at 18.87 min revealing a methylation metabolite of oroxin A. M43 was shown to have the chemical composition of C<sub>22</sub>H<sub>22</sub>O<sub>10</sub>, and was detected with the deprotonated ion at *m/z* 445.1142 under the mass conditions. Several representative ions at *m/z* 431.0535 and 269.0037 were detected through loss of CH<sub>2</sub> and C<sub>6</sub>H<sub>10</sub>O<sub>5</sub>. The individual retention time of M44 and M45 was at 19.20 and 19.48 min, which afforded deprotonated ions at *m/z* 299.0561 and 299.0570, a 30 Da increase from baicalein. This result suggests that an oxidation and methylation reaction happened from baicalein. The distinct ion at *m/z* 269.0619 was generated through loss of O and CH<sub>2</sub>. The chemical formula of M44 and M45 were inferred as C<sub>16</sub>H<sub>12</sub>O<sub>6</sub>. The respective calculated Clog P values were 2.36187 and 2.92187.

M46 was found at *m/z* 311.0561, whose mass was 42 Da more than that of baicalein. Moreover, M46 showed the elution time at 19.30 min, and the chemical composition was C<sub>17</sub>H<sub>12</sub>O<sub>6</sub>. The secondary fragment ion at *m/z* 269.0085 was found by loss of C<sub>2</sub>H<sub>2</sub>O, which suggested that it was an acetylation metabolite of baicalein. M47 was eluted at 21.92 min, and had the deprotonated ion at *m/z* 283.0612, 14 Da more than that of baicalein. The typical fragment ion at *m/z* 269.0656 ([M-CH<sub>2</sub>-H]<sup>-</sup>) and 241.0501 ([M-CH<sub>2</sub>-CO-H]<sup>-</sup>) suggested that M47 was the methylation metabolite of baicalein. In addition, the chemical composition of M47 was inferred as C<sub>16</sub>H<sub>12</sub>O<sub>5</sub>.

### 3.7. Metabolic pathways of main flavonoids

In this study, a multitude of metabolites have been discovered, with forty metabolites identified in rat blood, twenty-five metabolites in rat urine, twenty-five in rat bile, and thirty-seven in rat feces. Furthermore, the primary metabolic pathway involved

**Table 7**  
Mean extraction recoveries and matrix effects of ten flavonoids and IS in rat plasma (n = 6).

Compounds spiked concentration (ng/mL)	Extraction recovery		Matrix effect	
	Mean (%)	RSD (%)	Mean (%)	RSD (%)
Oroxin A				
2.52	88.71	3.45	87.06	3.76
1921.22	83.13	4.59	81.32	7.89
3115.94	85.77	2.88	92.17	5.44
Oroxin B				
2.24	81.09	3.09	101.5	6.53
1932.56	83.86	5.46	93.52	4.82
3282.62	84.73	3.84	93.16	6.59
Baicalin				
2.70	85.53	3.42	87.33	3.95
108.72	91.43	6.75	84.22	7.61
174.62	86.98	7.88	88.02	7.38
Chrysin				
2.50	86.47	2.64	93.32	4.93
73.98	86.84	4.45	87.29	5.32
116.20	92.65	7.86	96.74	6.26
Baicalein				
2.88	87.97	3.96	101.2	5.87
84.45	86.71	5.49	92.38	6.12
137.85	94.86	7.03	93.28	1.93
Scutellarein				
2.44	88.54	5.22	83.16	4.92
62.75	89.32	3.19	85.27	7.02
101.14	91.25	4.58	90.17	6.89
Apigenin				
2.04	86.38	6.49	82.72	5.54
98.66	89.03	5.98	79.99	7.88
158.67	85.91	6.29	101.3	6.22
Quercetin				
2.38	92.76	3.22	88.31	6.34
33.06	87.18	5.36	82.19	5.03
53.86	90.04	4.79	84.02	7.15
Oroxylin A				
2.64	85.08	5.24	87.04	6.27
51.96	86.97	7.69	85.97	5.26
84.20	84.06	5.94	92.18	4.77
Isorhamnetin				
2.06	89.87	6.93	83.71	5.33
76.14	93.48	5.49	82.48	7.43
122.66	86.06	7.63	97.09	5.87
Sulfamethoxazole(IS)	97.28	3.59	96.57	4.38
476				

conjugation reactions encompassing 25 metabolites (methylation, glucuronide, acetylation, sulfate, and glycine conjugation metabolites). The potential metabolic pathways of the main flavonoids *in vivo* were proposed as depicted in Supplementary material (Fig. S1-4).

### 3.8. Method validation for PK study

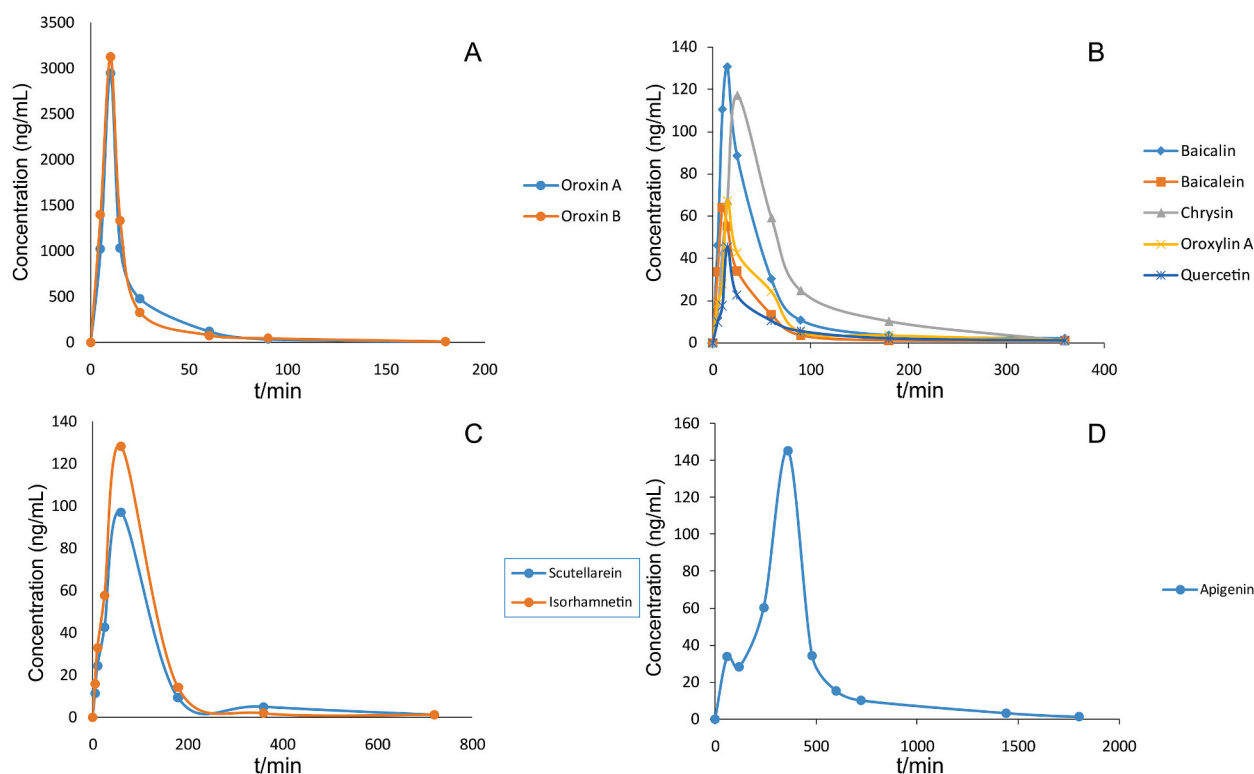
The MRM chromatograms of blank rat plasma, blank plasma spiked with the analytes and IS and plasma samples at 15 min after oral administration of *Oroxylum indicum* (L.) Kurz extract are shown in Fig. 6. The correlation coefficients calculated from the standard curves of analytes were all above 0.9969, indicating excellent linear correlations (Table 4). Table 5 displayed the intra- and inter-day precisions and accuracies (LLOQ, low, medium and high QC sample) for ten analytes. The RSD values of intra-day precision ranged from 3.04 % to 6.88 %, while those for inter-day precision range from 3.58 % to 8.34 %. The results of post-preparative stability, short-term temperature stability, long-term stability and freeze-thaw stability are shown in Table 6. The results suggested that all the analytes were stable under the storage conditions. The results of the recovery and matrix effect of ten analytes are summarized in Table 7. The average extraction recoveries of the QC samples ranged from 81.09 % to 94.86 %, and the RSD values were less than 7.88 %. Furthermore, the matrix effects fell within a range of 79.99%–101.5 %.

### 3.9. PK study of ten compounds in *Oroxylum indicum* (L.) Kurz extract

The developed HPLC-ESI-MS/MS method was successfully validated and applied to simultaneously determine concentrations of ten active chemical compounds in rat plasma following oral administration of *Oroxylum indicum* (L.) Kurz extract. The pharmacokinetic

**Table 8**Pharmacokinetic parameters of ten chemical compounds in rat plasma after single oral administration of *Oroxylum indicum* (L.) Kurz extract (n = 6).

Compounds	C <sub>max</sub> (ng/mL) (mean ± SD)	T <sub>max</sub> (min)	T <sub>1/2</sub> (min)	AUC <sub>0-t</sub> (ng/L • min) (mean ± SD)	AUC <sub>0-∞</sub> (ng/L • min) (mean ± SD)	CL (L/min/kg)
Oroxin A	2945.1 ± 11.23	10 ± 0.38	17.01 ± 0.14	85437.46 ± 16.11	85459.05 ± 23.77	130.65
Oroxin B	3123.9 ± 16.37	10 ± 0.67	41.08 ± 0.26	112256.52 ± 28.06	112856.89 ± 57.04	95.41
Baicalin	130.40 ± 27.52	15 ± 0.48	20.87 ± 0.42	6319.89 ± 28.81	6336.45 ± 33.24	2355.89
Chrysin	117.20 ± 28.54	30 ± 0.49	51.69 ± 0.53	8922.55 ± 37.73	8999.56 ± 59.51	2074.73
Baicalein	64.12 ± 19.33	10 ± 0.28	19.52 ± 0.35	2883.12 ± 44.29	2887.32 ± 57.28	4907.43
Scutellarein	97.22 ± 24.27	60 ± 0.37	177.89 ± 0.49	11956.49 ± 49.46	12257.3 ± 60.12	1408.99
Apigenin	145.22 ± 29.92	360 ± 0.25	434.88 ± 0.62	40925.96 ± 47.47	41413.20 ± 55.15	332.21
Quercetin	45.19 ± 18.84	15 ± 0.47	48.09 ± 0.39	2178.75 ± 55.84	2189.8939.97	8224.87
Oroxylin A	67.32 ± 15.78	15 ± 0.53	43.27 ± 0.21	3540.06 ± 59.51	3552.50 ± 56.01	4741.76
Isorhamnetin	128.44 ± 26.42	60 ± 0.22	68.62 ± 0.73	14854.32 ± 67.05	14859.74 ± 69.12	1121.47

**Fig. 7.** Mean plasma concentration-time curves of ten analytes after oral administration of *Oroxylum indicum* (L.) Kurz. (A) Oroin A and Oroxin B; (B) Baicalin, Baicalein, Chrysin, Oroxylin A and Quercetin; (C) Scutellarein and Isorhamnetin; (D) Apigenin.

parameters are listed in Table 8. And, the mean plasma concentration-time profiles of the investigated ten components are shown in Fig. 7 (A-D). The plasma concentrations of oroxin B (Fig. 7A) and quercetin (Fig. 7B) exhibited the highest and lowest level, respectively, which was consistent with the highest content of oroxin B and the lowest content of quercetin in the extract. Furthermore, a double-peak phenomenon of apigenin is depicted in Fig. 7D. The initial peak occurred at approximately 5 min, followed by a second peak at around 360 min, which exhibited a greater intensity than the first peak. This observation suggested a potential association with entero-hepatic recirculation. However, further investigation is required to validate this hypothesis. Overall, these findings provided valuable insights for further studies on the pharmacokinetics of *Oroxylum indicum* (L.) Kurz, facilitating its clinical application as a herbal medicine.

#### 4. Conclusions

The present study established a novel MSOP method based on the orthogonality of mass spectrum signals to eliminate the

interference from prototype compounds *in vivo*. Firstly, the validity and feasibility of the method were verified using a reference sample. The results showed that the MSOP method could effectively obtain the signal of metabolites. A total of 47 metabolites were identified in plasma, bile, urine and feces samples following oral administration of *Oroxylum indicum* (L.) Kurz extract. Specifically, 40 metabolites were detected in blood samples, while urine, bile, and feces samples contained 38, 24, and 37 metabolites respectively. Importantly, this study reported the pharmacokinetics of major compounds derived from *Oroxylum indicum* (L.) Kurz in rat plasma. The proposed method satisfactorily complies with the regulatory requirements for bioanalytical method validation. Furthermore, it was observed that scutellarein, apigenin and isorhamnetin slowed attainment of  $C_{max}$  levels. Conversely, oroxin A, oroxin B, baicalin, baicalein, quercetin and oroxylin A showed rapid absorption into blood circulation. These pharmacokinetic parameters along with plasma concentration-time profiles provided valuable insights for pre-clinical and clinical investigations regarding medical compound disposition.

## Data availability

Data will be made available on request.

## CRedit authorship contribution statement

**Xia Zhang:** Writing – review & editing, Writing – original draft. **Yuan Zhang:** Formal analysis. **Na Wang:** Software. **Jian Liu:** Validation. **Lan-tong Zhang:** Resources. **Zhi-qing Zhang:** Funding acquisition. **De-qiang Li:** Funding acquisition.

## Declaration of competing interest

The authors declare that they have no known competing financial interests or personal relationships that could have appeared to influence the work reported in this paper.

## Acknowledgements

This research was supported by the Natural Science Foundation of Hebei Province in China (H2023206050), Clinical Medicine Excellent Talent Training Program of Hebei Province in China (ZF2024031), the 14th Five-Year Plan Medical Innovation Research Team of Hebei Medical University (2022LCTD-B10) and the project of Hebei Administration of Traditional Chinese Medicine (No. 2021147).

## Appendix A. Supplementary data

Supplementary data to this article can be found online at <https://doi.org/10.1016/j.heliyon.2024.e33234>.

## References

- [1] A.C. Cardoso Reis, G.M. Valente, B.M. Silva, C.L.B. Magalhaes, M. Kohlhoff, G.C. Brandao, Anti-arboviral activity and chemical characterization of hispidulin and ethanolic extracts from *Millingtonia hortensis* L.f. and *Oroxylum indicum* (L.) Kurz (Bignoniaceae), *Nat. Prod. Res.* 37 (2022) 613–617.
- [2] J.B. Wen, Q.W. Zhang, Z.Q. Yin, Y.P. Li, X.W. Han, W.C. Ye, Flavonoids from the seeds of *Oroxylum indicum* (L.) vent, *Chin. Pharmaceut. J.* 46 (2011) 170–173.
- [3] R. Wang, M. He, X.C. Yuan, B. Jiang, M. Xue, Antioxidant activity of total flavonoids from *Oroxylum indicum*, *Chin. J. Exp. Tradit. Med. Formulae* 18 (2012) 102–105.
- [4] K. Lalrinzuali, M. Vabeiryureilai, C.J. Ganesh, Topical application of stem bark ethanol extract of Sonapatha, *Oroxylum indicum* (L.) Kurz accelerates healing of deep dermal excision wound in Swiss albino mice, *J. Ethnopharmacol.* 227 (2018) 290–299.
- [5] B. Dinda, I. SilSarma, M. Dinda, P. Rudrapaul, *Oroxylum indicum* (L.) Kurz, an important Asian traditional medicine: from traditional uses to scientific data for its commercial exploitation, *J. Ethnopharmacol.* 161 (2015) 255–278.
- [6] R.Y. Yan, Y.Y. Cao, Antioxidant flavonoids from the seed of *Oroxylum indicum*, *Fitoterapia* 82 (2011) 841–848.
- [7] D. Rai, H.N. Aswatha Ram, K. Neeraj Patel, U.V. Babu, L.M. Sharath Kumar, R. Kannan, *In vitro* immuno-stimulatory and anticancer activities of *Oroxylum indicum* (L.) Kurz.: an evidence for substitution of aerial parts for conservation, *J. Ayurveda Integr. Med.* 13 (2022) 100523.
- [8] J. Prapaipittayakhun, S. Boonyuen, A.L.T. Zheng, K. Apinyauppatham, P. Arpornmaeklong, Biologic effects of biosynthesized *Oroxylum indicum*/silver nanoparticles on human periodontal ligament stem cells, *OpenNano* 9 (2023) 100117.
- [9] S.S. Ahmed, M.O. Rahman, A.S. Alqahtani, N. Sultana, O.M. Almarfadi, M.A. Ali, J. Lee, Anticancer potential of phytochemicals from *Oroxylum indicum* targeting Lactate Dehydrogenase A through bioinformatic approach, *Toxicol Rep* 10 (2023) 56–75.
- [10] B.W. Zhang, Y.B. Sang, W.L. Sun, H.S. Yu, B.P. Ma, Z.L. Xiu, Y.S. Dong, Combination of flavonoids from *Oroxylum indicum* seed extracts and acarbose improves the inhibition of postprandial blood glucose: *in vivo* and *in vitro* study, *Biomed. Pharmacother.* 91 (2017) 890–898.
- [11] P. Mangal, P. Khare, S. Jagtap, M. Bishnoi, K.K. Kondepudi, K.K. Bhutani, Screening of Ayurvedic medicinal plants for anti-obesity potential: an investigation on bioactive constituents from *Oroxylum indicum* (L.) Kurz bark, *J. Ethnopharmacol.* 197 (2017) 138–146.
- [12] Z.Y. Liu, Y. Zhang, L.Q. Gu, X.H. Chen, Promotion of classic neutral bile acids synthesis pathway is responsible for cholesterol-lowering effect of Si-miao-yong-an decoction: application of LC–MS/MS method to determine 6 major bile acids in rat liver and plasma, *J. Pharmaceut. Biomed.* 135 (2017) 167–175.
- [13] S.S. Su, G.R. Xue, J.W. Shang, P.F. Yan, J.X. Wang, C.Y. Yan, J.X. Li, X. Xiong, H.J. Xu, Computational method for rapid screening of the metabolites of *Pulsatilla chinensis* in rats using UHPLC-Q-TOF/MS combined with mass spectrum-based orthogonal projection, *J. Pharmaceut. Biomed.* 229 (2023) 115345.
- [14] H. Wang, Y.T. Sun, W. Guo, J. Wang, J.Y. Gao, W.W. Peng, J.K. Gu, Identification and high-throughput quantification of baicalein and its metabolites in plasma and urine, *J. Ethnopharmacol.* 301 (2023) 115853.

- [15] M.T. Zhu, S.W. Lv, Y.P. Sun, G.Y. Li, B.Y. Yang, Q.H. Wang, H.X. Kuang, Characterization of metabolites of five typical saponins from *Caulophyllum robustum* Maxim and their biotransformation in fibroblast-like synoviocytes by UHPLC-Q-Exactive-Plus-Orbitrap-MS, *Arab. J. Chem.* 16 (2023) 104757.
- [16] M. Novak, B. Svobodova, J. Konecny, A. Kuratkova, L. Nevasadova, L. Prchal, J. Korabecny, V.M. Lauschke, O. Soukup, R. Kučera, UHPLC-Orbitrap study of the first phase tacrine in vitro metabolites and related Alzheimer's drug candidates using human liver microsomes, *Analysis* 225 (2023) 115154.
- [17] R.L. Xie, Y.P. Xu, M. Ma, X.D. Wang, L. Zhang, Z.J. Wang, First metabolic profiling of 4-n-nonylphenol in human liver microsomes by integrated approaches to testing and assessment: metabolites, pathways, and biological effects, *J. Hazard Mater.* 447 (2023) 130830.
- [18] C.A. Montilla, S. Moroni, G. Moscatelli, D.M. Rocco, N. Gonzalez, J.M. Alcheh, F.G. Bournissen, Major benzimidazole metabolites in patients treated for Chagas disease: mass spectrometry-based identification, structural analysis and detoxification pathways, *Toxicol. Lett.* 377 (2023) 71–82.
- [19] X. Shen, X. Li, C.F. Jia, J. Li, S.Y. Chen, B. Gao, W.K. Liang, L.B. Zhang, HPLC-MS-based untargeted metabolomic analysis of differential plasma metabolites and their associated metabolic pathways in reproductively anosmic black porgy, *Acanthopagrus schlegelii*, *Comp. Biochem. Physiol., Part D: Genomics Proteomics* 46 (2023) 101071.
- [20] J.Y. Wan, C.Z. Wang, Z. Liu, Q.H. Zhang, M.W. Musch, M. Bissonnette, E.B. Chang, L.W. Qi, C.S. Yuan, Determination of American ginseng saponins and their metabolites in human plasma, urine and feces samples by liquid chromatography coupled with quadrupole time-of-flight mass spectrometry, *J. Chromatogr. B* 1015 (2016) 62–73.
- [21] X. Zhang, Z.Q. Zhang, L.C. Zhang, K.X. Wang, L.T. Zhang, D.Q. Li, The development and validation of a sensitive HPLC-MS/MS method for the quantitative and pharmacokinetic study of the seven components of *Buddleja lindleyana* Fort, *RSC Adv.* 11 (2021) 26016.
- [22] Y. Zheng, G. Lui, S. Boujaafar, R. Aboura, N. Bouazza, F. Foissac, J.M. Treluyer, S. Benabound, D. Hirt, I. Gana, Development of a simple and rapid method to determine the unbound fraction of dolutegravir, raltegravir and darunavir in human plasma using ultrafiltration and LC-MS/MS, *J. Pharmaceut. Biomed.* 196 (2021) 113923.
- [23] C. Marchioni, I.D. Souza, V.R.A. Junior, J.A.S. Crippa, V. Tumas, M.E.C. Queiroz, Recent advances in LC-MS/MS methods to determine endocannabinoids in biological samples: application in neurodegenerative diseases, *Anal. Chim. Acta* 1044 (2018) 12–28.
- [24] J.M. Li, A.X. Huang, L. Yang, P. Li, W. Gao, A sensitive LC-MS/MS method-based pharmacokinetic study of fifteen active ingredients of Yindan Xinnaotong soft capsule in rats and its potential mechanism in the treatment of cardiovascular diseases, *J. Chromatogr. B* 1220 (2023) 123663.
- [25] C.Y. Ma, N. Sheng, Y.Y. Li, H. Zheng, Z. Wang, J.L. Zhang, A comprehensive perspective on the disposition, metabolism, and pharmacokinetics of representative multi-components of Dengzhan Shengmai in rats with chronic cerebral hypoperfusion after oral administration, *J. Ethnopharmacol.* 307 (2023) 116212.
- [26] Y.T. Wang, X. Sun, J.W. Qiu, A. Zhou, P.B. Xu, Y.R. Liu, H.F. Wu, A UHPLC-Q-TOF-MS-based serum and urine metabolomics approach reveals the mechanism of Gualou-Xiebai herb pair intervention against atherosclerosis process in ApoE<sup>-/-</sup> mice, *J. Chromatogr. B* 1215 (2023) 123567.
- [27] Z.Y. Zhang, P.P. Jia, X.X. Zhang, Q.Y. Zhang, H.T. Yang, H. Shi, L.T. Zhang, LC-MS/MS determination and pharmacokinetic study of seven flavonoids in rat plasma after oral administration of *Cirsium japonicum* DC. Extract, *J. Ethnopharmacol.* 158 (2014) 66–75.
- [28] C.J. Liang, J.T. Yin, Y.H. Ma, X. Zhang, L.T. Zhang, Quantitative determination of characteristic components from compound of *Lysionotus pauciflorus* Maxim. by LC-MS/MS and its application to a pharmacokinetic study, *J. Pharmaceut. Biomed.* 177 (2020) 112835.
- [29] C.J. Liang, X. Zhang, X.P. Diao, M. Liao, Y.P. Sun, L.T. Zhang, Metabolism profiling of nevadensin in vitro and in vivo by UHPLC-Q-TOF-MS/MS, *J. Chromatogr. B* 1084 (2018) 69–79.
- [30] L.W. Chen, N.N. Wei, Y. Jiang, C.Y. Yuan, L.W. Xu, J.D. Li, M. Kong, Y. Chen, Q. Wang, Comparative pharmacokinetics of seven bioactive components after oral administration of crude and processed Qixue Shuangbu Prescription in chronic heart failure rats by microdialysis combined with UPLC-MS/MS, *J. Ethnopharmacol.* 303 (2023) 116035.
- [31] W.T. Wang, Z.H. Zheng, J.Y. Chen, T.T. Duan, H.Y. He, S.J. Tang, Characterization of metabolite landscape distinguishes wild from cultivated *Polygonati Rhizomes* by UHPLC-Q-TOF-MS untargeted metabolomics, *Food Biosci.* 24 (2023) 102574.
- [32] B.B. Ge, X.J. Wang, W. Li, Y.M. Du, T.F. Ji, G.H. Du, C.Y. Fang, J.H. Wang, A sensitive LC-MS method for the determination of Sinomenine derivative SWX and its application to pharmacokinetic research in rats, *J. Chromatogr. B* 1213 (2022) 123474.
- [33] P.A. Markin, N.E. Moskaleva, S.A. Lebedeva, S. Kozin, E.M. Grigorevskikh, L.G. Kolik, T.A. Gudasheva, S.A. Appolonova, LC-MS/MS determination of GTS-201, a dipeptide mimetic of the brain-derived neurotrophic factor, and neurotransmitter metabolites with application to a pharmacokinetic study in rats, *Analysis* 223 (2023) 115125.
- [34] X.W. Shi, Y.B. Wu, T. Lv, Y.F. Wang, Y. Fu, M.M. Sun, Q.W. Shi, C.H. Huo, Q. Wang, Y.C. Gu, A chemometric-assisted LC-MS/MS method for the simultaneous determination of 17 limonoids from different parts of *Xylocarpus granatum* fruit, *Anal. Bioanal. Chem. Re.* 409 (2017) 4669–4679.
- [35] M.L. Zhang, L.Q. Luo, X.Y. Dai, Y.F. He, J.S. Ma, Determination of oleandrin and adynerin in rat plasma by UPLC-MS/MS and their pharmacokinetic study, *Arabian J. Chem.* 15 (2022) 104369.
- [36] H.Y. Mou, Orthogonal Projection Method Based on Mass Spectrum Signal and Its Application in Metabonomics of Traditional Chinese Medicine Application, Univ. Suzhou, 2012.